Physiology of Camptothecin Synthesis in Plants and Root Organ Cultures of *Ophiorrhiza mungos* L. and Its Production in Root Fermenters

Bernhard Wetterauer, Eric Hummel, Steffen Walczak, Melanie Distl, Markus Langhans, Pille Wetterauer, Frank Sporer, Eckhart Wildi, and Michael Wink

Abstract Production of the anticancer drug camptothecin (CPT) was examined in *Ophiorrhiza mungos* with regard to concentration and localization of CPT and CPT derivatives within all plant parts. First, morphology and histology studies of all organs were examined by light and confocal laser scanning microscopy to localize the accumulation of CPTs down to the subcellular level. In addition, CPTs were analysed qualitatively and quantitatively in all parts of a young and adult plant. A reverse distribution of CPT and 9-methoxycamptothecin (9-methoxy CPT) in the aerial parts became obvious,

Authors Eric Hummel and Steffen Walczak have been equally contributed to this chapter.

B. Wetterauer (✉) · P. Wetterauer · F. Sporer · M. Wink
Institute of Pharmacy and Molecular Biotechnology (IPMB), Heidelberg University, Heidelberg, Germany
e-mail: bernhard.wetterauer@urz.uni-heidelberg.de; p.wetterauer@urz.uni-heidelberg.de; frank.sporer@gmx.de; wink@uni-heidelberg.de

E. Hummel
Carl Zeiss Microscopy GmbH, Munich, Germany
e-mail: eric.hummel@zeiss.com

S. Walczak
Brooks Automation GmbH, Radolfzell, Germany
e-mail: swalczak@gmx.de

M. Distl
Formerly Institute of Pharmacy and Molecular Biotechnology (IPMB), Heidelberg University, Heidelberg, Germany

M. Langhans
Ernst-Berl-Institut, Macromolecular Chemistry & Paper Chemistry, Darmstadt Technical University, Darmstadt, Germany
e-mail: langhans@bio.tu-darmstadt.de

E. Wildi
Merz Pharma AG (formerly ROOTec GmbH, Heidelberg, Germany), Allschwil, Switzerland
e-mail: eckhart.wildi@merz.ch

S. Malik (ed.), *Exploring Plant Cells for the Production of Compounds of Interest*, https://doi.org/10.1007/978-3-030-58271-5_11

localized predominantly in the vacuoles of evenly distributed cells of the outer parenchymal tissues. On an average, the young plant contained 795 µg CPTs/g DW and the old plant 1182 µg CPTs/g DW. The plant roots contain only CPT, mainly localized in the rhizodermis and exodermis (866–1853 µg/g DW or 180–433 µg/g FW). The highest contents of CPTs were detected in the youngest leaves of the young plant (about 1664 µg/g DW or 304 µg/g FW; 60% 9-methoxy CPT), in the ripening seed capsules of the adult plant (1688 µg/g DW), and its oldest leaves (2000 µg/g DW). The average 9-methoxy CPT content in the aerial plant parts of the young and old one was about 490–600 µg/g DW and 68–81 µg/g FW, respectively. The storage in aerial parts shows a classical protection and defence pattern against herbivores. The epidermally localized CPT of the roots is partly released in the surroundings for an allelopathic purpose.

CPT localization and storage differed in root organ cultures from those in plants. CPT distribution within the root tissues of the untransformed and the transformed root organ culture line 607 and the occurrence of CPT in root tip exudates were investigated. Surprisingly, CPT was dispersed equally in both root culture lines, independent of age and part, but in relation to the dry biomass. The root tip exudates showed calcium oxalate crystals with embedded CPT. Additional elicitor studies on root cultures with many simple and complex elicitors, as well as precursors and physical/chemical stressors, did not stimulate CPT production. Therefore, the CPT biosynthesis in *O. mungos* seems to be constitutive and developmentally regulated.

Finally, preliminary scale-up experiments with transformed and untransformed root organ cultures in a mist fermenter were conducted, showing that a CPT production on a larger scale by root organ cultures of *O. mungos* is feasible.

Keywords 9-Methoxycamptothecin · Anticancer drug · Camptothecin · Elicitation · Fermenter · Localization · *Ophiorrhiza mungos* · Regulation · Root organ cultures · Storage

Abbreviations

2,4-D	2,4-Dichlorophenoxyacetic acid
9-Methoxy CPT	9-Methoxycamptothecin
CPT	Camptothecin
DMSO	Dimethyl sulfoxide
DW	Dry weight
ER	Endoplasmic reticulum
FAA	Formalin-acetic acid-alcohol
FW	Fresh weight
MeJA	Methyl jasmonic acid
PDA	Photodiode array
rpm	Revolutions per minute
SA	Salicylic acid
STR	Strictosidine synthase
TDC	Tryptophan decarboxylase
TIC	Total ion current

1 Introduction

Since the discovery of camptothecin (CPT) by Wall and Wani (Wall et al. 1966), CPT has led to medicinal research with many ups and downs resulting in chemotherapeutical agents of high efficacy like irinotecan, topotecan, and others (e.g. Oberlies and Kroll 2004). Additionally, CPT and its derivatives show other interesting applications with antiviral, antiparasitic, pesticidal, and antipsoriatic activities (reviewed in Liu et al. 2015), as a plant growth regulator (e.g. Buta and Worley 1976; Wang et al. 1980), or in traditional medicines against bites by snakes and rabid dogs, for treatment of stomatitis and ulcers, and for wound healing (Anaswara Krishnan et al. 2014). This broad spectrum of use is attributed to the two modes of action hither to known for CPT. Firstly, CPT inhibits the DNA topoisomerase I and thus replication, which was elucidated by Hsiang et al. (1985), and secondly, it binds to tubulin and therefore inhibits the microtubule formation in dividing cells, as shown recently by Wang et al. (2016) in our lab.

CPT is biosynthesized by different plant species of diverse plant families in the Asterids (APG III; Wink 2003). As already described by Li and Adair (1994), CPT is obtained as a raw material for the chemical industry mainly by cultivation of *Camptotheca acuminata* Decaisne and related species in plantations in China, India, further southeastern Asian countries, and North America (see also Liu and Adams 1996; Liu et al. 1999; Sirikantaramas et al. 2007a). But also natural sources are exploited by collections of *C. acuminata*, *Nothapodytes* spec., and other plants. In the producing countries, no environmental conservation legislation exists for the most part and the labour costs are minimal; otherwise, the actual low market prices of CPT would not be possible (≥3500 €/kg). At the moment, it seems that the supply of the pharmaceutical industry with CPT and CPT derivatives as raw material poses no problem, especially on examination of the sinking market prices in the last two decades and the CPT bulk (Wetterauer et al. 2018). However, this might be an illusion in a long-term view (Nagesha et al. 2018). In the last few decades, many investigations have been done in the field of chemistry and biotechnology to establish sustainable and ecologically compatible ways of CPT production and to become more independent from the classical sources (Wetterauer et al. 2018). However, until now, no breakthrough has taken place, mostly for economic reasons. In our case, we described a running and cost-effective system of root organ cultures of *Ophiorrhiza mungos* L. (Rubiaceae) that was developed together with the ROOTec company in the early 2000s (Wink et al. 2005; Wink and Wetterauer 2019). But in the end, the pharmaceutical industry showed no interest to use this technology, so expectations should be realistic.

Nevertheless, there are two other gaps of knowledge in this field. On the one hand, the anabolic pathway of the biosynthesis of CPT and its derivatives has not been completely elucidated until now. In this connection, the so-called ‘poststrictosamide events’ are mainly affected (e.g. Asano et al. 2013). Therefore, the biotechnological possibilities, like genetically engineered bacterial or yeast cultures, cannot be fully exploited at present for the bio-production of the highly

valuable CPT. On the other hand, many studies have been carried out for CPT content and derivate analyses in CPT-producing plants (comp. overview in Wetterauer et al. 2018), but very little is known about the regulation of their CPT biosynthesis, the cellular and subcellular localization of CPT, or its manner of storage and content regulation. To obtain more information about these questions, deep transcriptome analysis coupled to untargeted metabolomic profiling was performed by Yamazaki et al. (2013) in *O. pumila*, which did lead to new hints, but unfortunately not to clearer findings.

In the present study, we compiled the results of our investigations on *O. mungos* plant and root organ cultures over many years, focussing on the content of CPTs; their storage at the organ, tissue, and subcellular level; and regulation in relation to function and potential productivity for CPT bio-production. In doing this, we performed intensive confocal laser scanning microscopy studies and CPT content determinations by LC-MS/MS for root organ cultures and on intact plants. To stimulate the CPT production in transformed and untransformed root organ cultures, extensive elicitor studies were conducted. Finally, the results of the first fermenter studies of transformed and untransformed root organ cultures with respect to the CPT production, nutrition, and growth parameters are shown. The challenges of scaling up a root fermenter system are discussed as well.

2 Material and Methods

2.1 Plant Material and Culture Conditions

Ophiorrhiza mungos seeds were obtained from the Old Botanical Garden of Göttingen, Germany. The primary roots of germinating seeds were taken in a sterile cultivation regime of plates and shaking cultures. By transformations of primary roots, root organ shaking cultures, and stem axis parts by means of underpressure infiltration with different *Agrobacterium rhizogenes* strains (LBA 9402, Atcc 15834, and TR 105), ROOTec GmbH (Heidelberg, Germany) cultivated 23 lines of root organ cultures with individual characteristics with regard to vitality, growth behaviour, and CPT biosynthesis (see also Wetterauer et al. 2018). The mainly investigated root culture line 607 was transformed with the *A. rhizogenes* strain LBA 9402 by underpressure infiltration of a primary root. Transformation controls were carried out as described in Wetterauer et al. (2018).

The cultivation of the transformed and untransformed root organ cultures was conducted on plates by using a modified Gamborg B5 agar (0.4% Gelrite®, Carl Roth GmbH & Co., Karlsruhe, Germany) with 3% sucrose at 25 °C in the dark. The root organ shaking cultures of *O. mungos* were cultivated in modified Gamborg B5 medium (Gamborg et al. 1968) with 3% sucrose and ½ MS vitamins at a pH of 5.7 without hormone addition at 25 °C and 60 rpm on a rotary shaker in the dark.

Two adult plants of *O. mungos* were made available to us from the Old Botanical Garden of Göttingen, Germany, for first content studies. Identification of the plant species was performed by C. E. B. Bremekamp in September 1958 (personal communication with E. J. Gouda, curator of the Botanical Garden of Utrecht, Netherlands). These plants of *O. mungos* were integrated into the inventory of the Botanical Garden of Heidelberg under the accession number 108108 in October 2004. Herbarium vouchers were deposited at the Institute of Pharmacy and Molecular Biotechnology (IPMB) in November 2006 under the accession numbers P6984 and P6985.

Plant clones, for direct comparative studies, were grown out of young sprouts of the untransformed root plate cultures and cultivated on general soil substrate in the greenhouse at 20–25 °C and 80% air humidity. These plants were integrated in the Botanical Garden of Heidelberg, Germany, under the accession number 108181.

2.2 Histological Preparations

Fresh shoot cross sections of *O. mungos* were fixed in FAA, stepwise dehydrated in an ethanol and tertiary butanol series, embedded in Peel-A-Way® (Micro-cut paraffin, Polyscience Inc., Warrington PA, USA; melting point 56 °C) at 58 °C, cut with a Jung slide microtome at 10–12 μm, and stained with safranin O and fast green FCF (both obtained from Merck KGaA, Darmstadt, Germany). Leaves of *O. mungos* were not rigid enough and broke during the cutting by that method. For this reason, histological studies of the leaves were done in situ by ordinary microscopy and confocal microscopy. Roots were not treated in this way, because the histological structure became obvious in the confocal microscopy studies without any treatment.

2.3 Microscopy

All histological light microscopical examinations were done by an Axiovert inverted oil immersion microscope (Zeiss, Jena, Germany). The in situ localization studies of CPTs were performed by a confocal laser scanning microscope LSM 510 META (Zeiss, Jena, Germany).

2.4 CPT Localization by Confocal Laser Scanning Microscopy

All visual localizations of CPTs in situ were done by confocal laser scanning microscopy at 405 nm excitation wave length and 470 nm emission wave length. For excitation, a laser diode 405 nm was employed. Lambda scans were done from

417 to 748 nm in 10–11 nm steps (cf. Fig. 1). The evaluation of the measurements was done by LSM Image Browser Software (Zeiss, Jena, Germany).

For CPT, reference pure (*S*)-(+)-CPT (Sigma-Aldrich Chemie GmbH, Steinheim, Germany) was used, and for comparison, lambda scans were done continuously for all in situ tested tissues like exemplarily shown in Figs. 1 and 2. The emission minimum at 513 nm was a technical effect due to the main beamsplitter 405/514 of the used confocal laser scanning microscope.

Because of the suboptimal excitation wavelength of 405 nm, determined through the available laser diode, (371 nm for CPT and 9-methoxy CPT would be the best), the results are not perfect but a localization of the CPTs in the living tissues was possible. A differentiation of CPT and 9-methoxy CPT in spite of different emission maxima (for pure dissolved CPT at 435 nm and for 9-methoxy CPT at 502 nm in spectroscopic measurements) was also not possible. Therefore, only mixed results can be shown in the present work for the aerial parts of *O. mungos*, so that in the following, they are called simply CPTs.

2.5 Extraction Methods and Analytic Procedures

Quantitative Determination of CPT in Non-photosynthetic Tissues

For high-throughput screening, an extraction and spectroscopic method for tissues without chlorophyll (e.g. root, callus) was developed for quantitative determination of CPT based on its absorption maximum at 366 nm and emission wave length at 465 nm (96-well-plate reader GENIOS; Tecan Austria GmbH, Grödig/Salzburg, Austria). For this purpose, 10–12 mg of lyophilized and ground tissue samples were extracted with 1 ml MeOH twice. Purification was followed by addition of 500 µl KH_2PO_4 buffer (50 mM, pH 2.6) and two times shaking out with 500 µl CH_2Cl_2. After the combined organic layers were reduced to dryness, the remaining residues were dissolved in 1 ml MeOH. 100 µl was used for spectroscopic measurement in 96-well plates (FluoroNunc, black, F96, CC; Nalge Nunc International, Wiesbaden, Germany). For reader calibration, an external CPT solution series from 0 to 10 µg CPT/ml in MeOH was used. Qualitative and quantitative validations of this method were carried out by HPLC.

The CPT content in liquid medium samples was measured directly with the same spectroscopic method as described. As calibration standard, an external CPT solution series from 0 to 5 µg CPT/ml in Gamborg B5 culture medium was used. For more details, see Wetterauer et al. (2018).

Quantitative and Qualitative Determination of CPT and 9-Methoxy CPT Contents in Photosynthetic Tissues by LC-MS/MS

In the case of chlorophyll-containing tissues or the qualitative determination of CPTs in tissues not previously investigated, a determination of the CPT contents was carried out by LC-MS/MS. The extraction method for tissue samples was

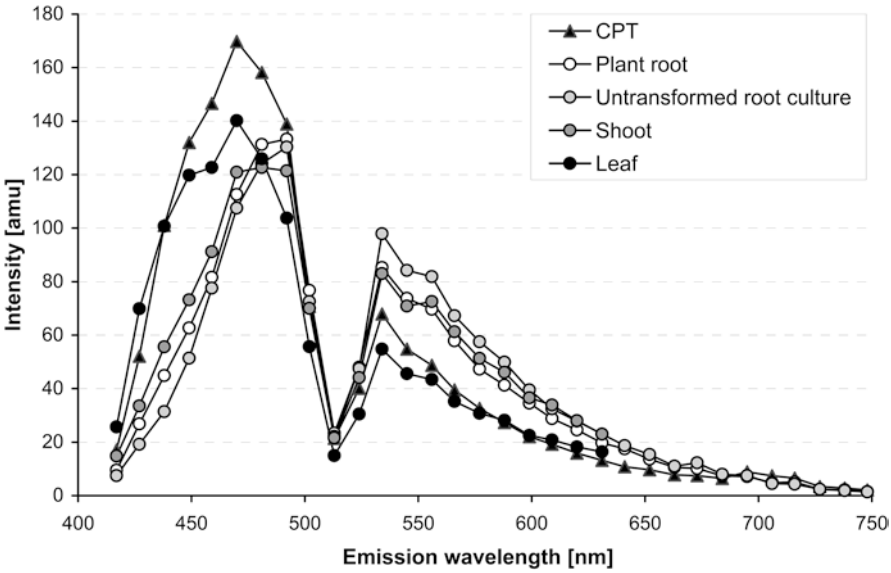

Fig. 1 Lambda scans of selected fluorescent vacuoles in different living tissues of *Ophiorrhiza mungos* plant and root organ cultures in comparison to pure CPT (cf. Fig. 2) at 405 nm excitation wavelength using emission filters 417, 427, 438, 449, 459, 470, 481, 492, 502, 513, 524, 534, 545, 556, 566, 577, 588, 599, 609, 620, 631, 641, 652, 663, 673, 684, 695, 706, 716, 727, 738, and 748 nm

conducted in the same way as described before for the non-photosynthetic tissues. Medium samples were analysed directly without any treatment.

LC-MS/MS analysis was carried out on a Finnigan LCQ-Duo ion trap mass spectrometer with an ESI source (ThermoQuest, San Jose, CA, USA) connected to a Finnigan Surveyor HPLC system (MS pump plus, autosampler, and PDA detector plus) (Thermo, San Jose, CA, USA) with an EC 150/3 Nucleodur 100-3 C18ec column (Macherey-Nagel, Düren, Germany). A gradient of water and acetonitrile (ACN) (with 1% formic acid each) was applied from 10 to 50% ACN in 20 min at 30 °C. The flow rate was 0.5 ml/min. The injection volume was 20 µl. All samples were measured in the positive mode. The MS was operated with a capillary voltage of 10 V, source temperature of 240 °C, and high purity nitrogen as a sheath and auxiliary gas at a flow rate of 80 and 40 (arbitrary units), respectively. The ions were detected in a mass range of 50–2000 m/z. The collision energy of 35% was used in MS2 for fragmentation. Data acquisitions and analyses were carried out by Xcalibur™ 2.0.7 software (Thermo Scientific, Karlsruhe, Germany).

As external calibration, a combined standard of CPT (Sigma-Aldrich Chemie GmbH, Steinheim, Germany) and 9-methoxy CPT (Chengdu Biopurify Phytochemicals Ltd., Chengdu, Sichuan, China) dissolved in MeOH was used (concentrations of CPT/9-methoxy CPT: 0.47/0.50, 4.65/5.05, 23.25/25.23, and 46.50/50.45 µg/ml). An example of an *O. mungos* leaf sample is given in Fig. 3.

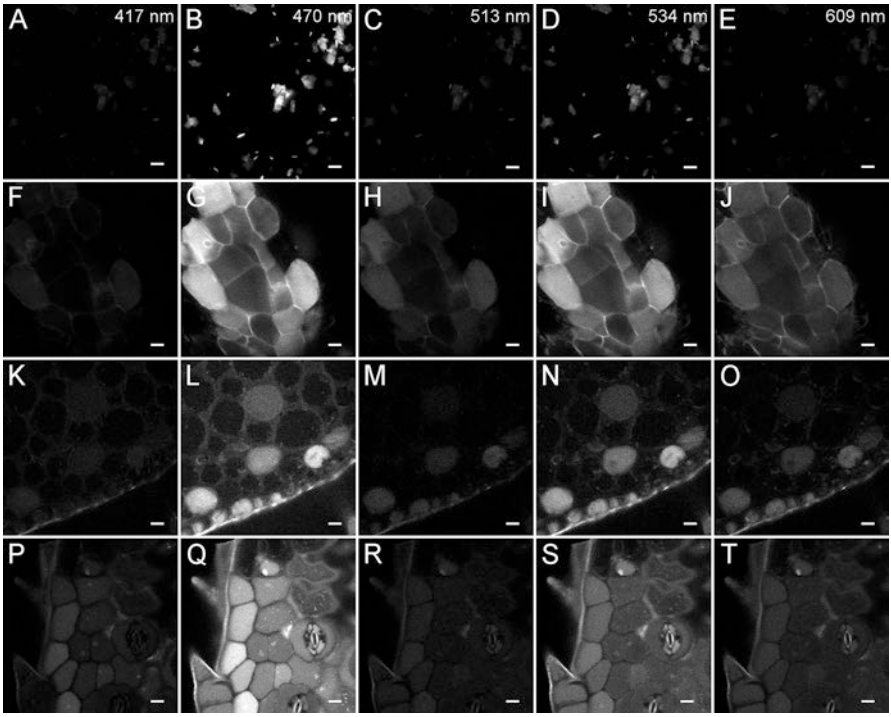

Fig. 2 Confocal laser scanning microscopy fluorescence images of selected wavelengths (minima and maxima) of lambda scans (cf. Fig. 1) of CPT standard (**a–e**) (CPT crystals measured in 1 µl slideVI flow chamber for cell microscopy, ibidi GmbH, Munich, Germany), differentiated rhizodermis of the plant root of *Ophiorrhiza mungos* (**f–j**), epidermis and cortex parenchyma of a shoot cross section of *O. mungos* plant (**k–o**), and epidermis of the abaxial leaf surface with hairs of *O. mungos* (**p–t**). All samples were measured in Gamborg B5 medium at 405 nm excitation wavelength; all scale bars correspond to 10 µm

2.6 *Further Analyses of Root Organ Cultures of* Ophiorrhiza mungos

Studies on Root Tip Exudates

As known, root organ cultures of *O. mungos* release CPT in the culture medium (e.g. Wetterauer et al. 2018). On the culture plates, the transformed root cultures of *O. mungos* (Fig. 4a) grew in a unipolar fashion, and droplets of root exudate were observed hanging from the tips of roots growing in the air. Under light exposure of 366 nm, these droplets showed the same fluorescence as CPT. Therefore, we tried to investigate the CPT content in the root exudates (Fig. 4b).

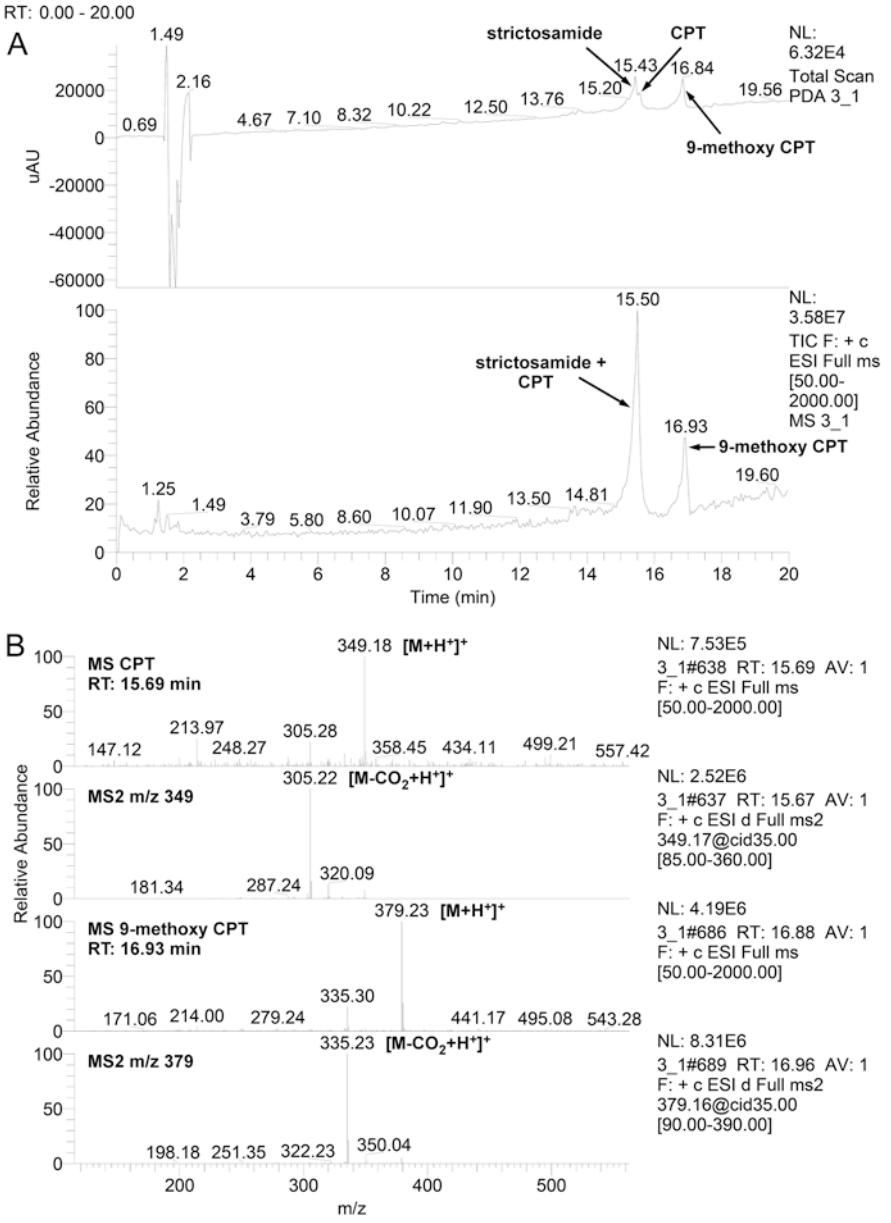

Fig. 3 LC-MS/MS analysis of an *Ophiorrhiza mungos* leaf sample. (**a**) PDA (200–600 nm) and TIC chromatograms of strictosamide, CPT, and 9-methoxy CPT; (**b**) MS and MS2 mass spectra of CPT and 9-methoxy CPT from the TIC of part A. For strictosamide, no mass spectra were shown (MS m/z 499.15 $[M + H^+]^+$, MS2 m/z 337.07 $[M\text{-}Glc + H^+]^+$) (compare Yamazaki et al. 2003b)

CPT Distribution in Transformed and Untransformed Root Organ Cultures

Four 7-week-old transformed (line 607) and untransformed root organ cultures each were cut into five equally thick parts from the youngest to the oldest tissue (Fig. 5) and each analysed for CPT content in relation to FW, DW, and DW density. After FW determination, all samples were frozen at − -80 °C, lyophilized, the DWs measured, and the CPT contents defined by the described standard method. The dry weight density was determined by measuring the volume of a defined amount of dry root powder with modified insulin syringes connected to a vacuum pump with maximum vacuum.

2.7 Elicitor Studies

Extensive elicitor studies on *O. mungos* root cultures [transformed (line 607) and untransformed] were performed to investigate whether a stimulation of CPT biosynthesis is possible or not. To this end, many different single elicitors, both simple (defined) and complex (defined and undefined), as well as precursors and abiotic physical and chemical stress conditions, were tested (Table 1). More detailed experimental conditions are described in Wetterauer (2008). Additionally, a combination of 0.1 mg/flask indole acetic acid (IAA) and 0.01 mg/flask kinetin was tested on untransformed root organ cultures with an inoculum size of 3.7 g ± 0.7 g (n = 3). Medium sampling for CPT content determination was done after 0, 5.5, 18.5, 26, 52, 75, 96.5, 145, and 193 h. At the end of the testing period, the roots were harvested, and the CPT content of the tissues was determined in different relations.

2.8 Fermenter

For our own studies and the optimization, or rather determination, of root growth and culture conditions for a stimulation of CPT formation during upscale, we built our own mist bioreactor (cf. Bastian et al. 2008). This test mist fermenter, called WEWA I, was based functionally on the Low Cost Mist Bioreactor (LCMB) of the ROOTec GmbH company (patents: US 2003/0129743A1; EP 1268743B1) (cf. Wink et al. 2005; Wink and Wetterauer 2019).

For scaling up a root culture system in the WEWA I, many factors had to be considered first. Of particular importance were the inoculum size and its dispersion on the gauze carrier; the nutrition concentrations in the culture medium (to avoid an osmotic shock or over-fertilization); the balance between spray volume, pressure, and cycle time; and, of course, the aspects of sampling and sterility.

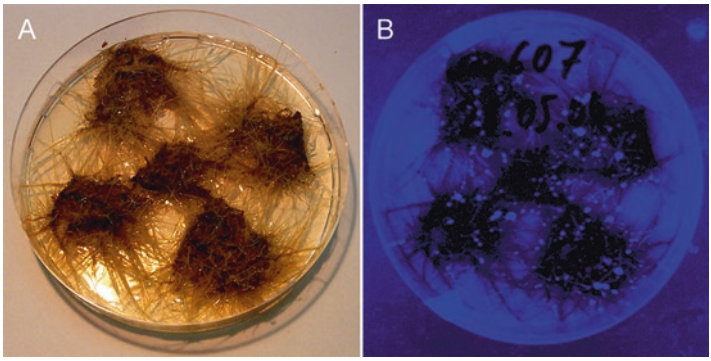

Fig. 4 Plate of the transformed root organ culture line 607 of *Ophiorrhiza mungos*: (**a**) Plate at daylight, (**b**) fluorescence exposure at an excitation wavelength of 366 nm. The culture agar and the root exudate droplets on the air growing root tips show the blue CPT fluorescence

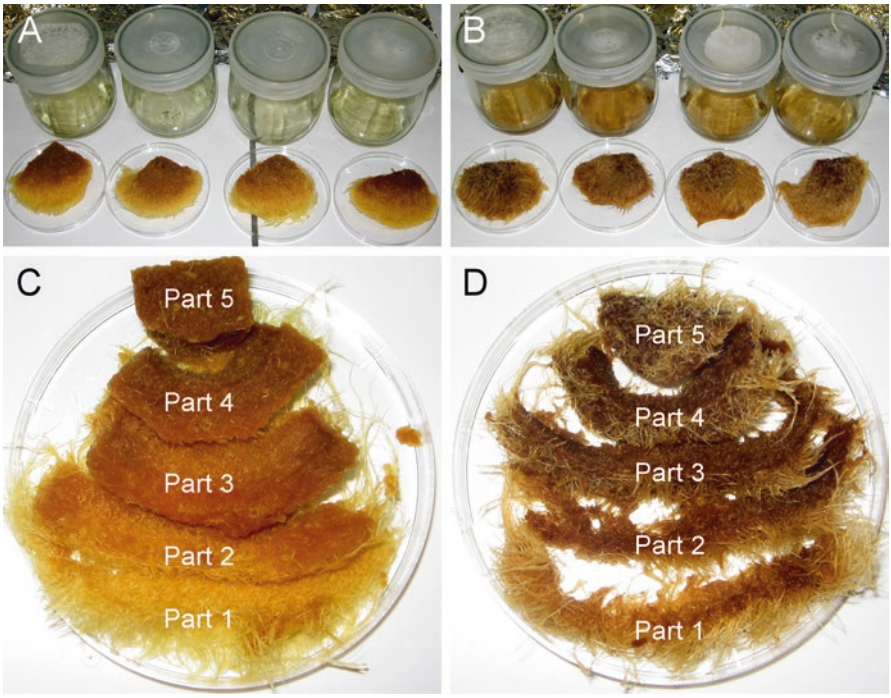

Fig. 5 Seven-week-old untransformed (**a**, **c**) and transformed (line 607, **b**, **d**) root organ cultures of *Ophiorrhiza mungos*. Cultures were cut into five equally thick parts from the root tips to the oldest tissues (**c**, **d**) for CPT analyses

The sterile even dispersion of the inoculum roots on the culture carrier (nylon gauze 250 µm; surface area approx. 185 cm^2) was the first challenge. As shown in the scheme of Fig. 6a, the assembly of the preparation device looks quite complex. A longer period of testing was necessary to obtain fairly good results. The root tips used for 6-week-old transformed or untransformed root cultures were harvested (length 1–1.5 cm) (Fig. 7a), dispersed in 3 litres of sterile B5 medium without sucrose by stirring (Fig. 7b), filled at once in the brass cylinder of the assembly, and placed on the gauze carrier by underpressure suction of the medium. In the testing phase, when the assembly was not sophisticated, the roots agglomerated quickly, as shown in Fig. 7c. The relevant factors here are pumping speed, dispersion volume, and linearity of the siphoning over the whole gauze area. After many modifications, the dispersion of the roots became better (Fig. 7d, e). Regarding the inoculum size at the beginning, 4 g FW of root tips were used (Fig. 7d). Over time we recognized that an inoculum of >20 g FW led to better vitality in the fermentation process (Fig. 7e).

Table 1 Elicitors, precursors, and abiotic stressors tested for amplification of the CPT biosynthesis in root organ cultures of *Ophiorrhiza mungos*

Simple elicitors

- Methyl jasmonic acid (1–1000 µM)
- Salicylic acid (0.01–1 µM)
- Methanol (0.05–5%)
- Ethanol (0.05–5%)
- Indole acetic acid (auxin) (0.1 mg) + kinetin (0.01 mg)
- Hydrogen peroxide (0.001–0.1%)
- Coniine (3 mM)
- Diethyldithiocarbamate (5 mM)
- Caffeine (1 mM)
- Quercetin (1 mM)
- Papaverine (1 mM)
- Tannin (1.7 mg)
- Spermine (1 mM)
- Spermidine (1 mM)
- cAMP (0.5 mM)

Complex elicitors

Defined

- Ionophore A23187 (0.025–2.5 µM)
- Nystatin (1–20 mg)
- Chitosan 86/30/A1 (10 mg)
- Chitosan lactate (10 mg)
- Carboxymethyl chitosan (10 mg)

Undefined

- Mycelium *Pythium aphanidermatum* CBS 101589 (10–100 mg DW)
- Fungal cell wall extract *Pythium aphanidermatum* CBS 101589 (100–1000 µl)
- Mycelium *Phytophthora cinnamomi* DSM 62654 (20 mg DW)
- Mycelium *Phytophthora drechsleri* DSM 62680 (20 mg DW)
- Mycelium *Pythium ultimum* DSM 62987 (20 mg DW)
- Mycelium *Ascochyta hordei* CBS 112524 (20 mg DW)
- Mycelium *Ascochyta hordei* var. *hordei* CBS 504.71 (20 mg DW)
- Self-elicitation: root organ cultures were elicited by fresh root cultures ground with a pestle (0.14–1.3 g FW)
- Orange juice (2% (v/v))
- Tomato puree (0.58 ± 0.11 g)

Precursors

- Tryptophan (1 mM)
- Tryptamine (1 mM)

Abiotic stressors

- pH value (3–9)
- Shaking conditions (60–110 rpm)

Also, the nutrient concentrations of the culture medium were important during scaling up, because of a different biomass-to-medium volume ratio. In all procedure, we had to avoid osmotic shock and a supply of excess nutrients. After many test series with root tips in 12-well plates for optimization (not shown), a half concentrated B5 medium with 0.5% sucrose was used in the first fermenter tests. For the prevention of bacterial or fungal contaminations, 0.5 g/l Claforan® (bacteriostatic activity) and 40 mg/l nystatin (fungicidal activity) were added to the culture medium.

The fermenter vessel (volume approx. 3 litres) and the medium reservoir (volume approx. 1.8 litres) were made out of stainless steel (Fig. 6b, d), further attachment parts out of brass. All gas and medium connections were PTFE tubes. The medium filter filled with glass wool, necessary to avoid solid clogging of the spray nozzle, was a special element made of glass, as was the resin column. In the gas inlet and outlet of the fermenter system, safety sterile filters (0.45 µm, ∅ 50 mm; neoLab®, Laborbedarf-Vertriebs GmbH, Heidelberg, Germany) were integrated. The spray nozzle was a modified brazen replica of the two-component nozzle Hago GSC long nose (DIVA Sprühtechnik GmbH/DELAVAN® Industriedüsen, Hamburg, Germany). The piloting of the four regulation magnetic valves (Typ D118V03-Z610A-2.7-230V AC, SIRAI Magnetventile Deutschland GmbH, Steinhöring, Germany) for the control of gas and medium flow were done by a home-made central processing unit (Fig. 6d bottom right).

The function principle of the WEWA I is based on gas pressure that can be divided into three phases (Fig. 8). The carrier gas was synthetic air (20% O_2, 80% N_2) with a pressure of 2 bars, which was responsible for all processes by control of the four valves. In phase I (spraying phase), valves 1 (medium inlet) and 2 (gas inlet) are opened and valves 3 (gas/pressure outlet) and 4 (medium outlet) are closed. The carrier gas drives the nozzle, and through the suction effect and the pressure being raised to that of the medium reservoir, the medium is pulled into the nozzle and sprayed out. In phase 2 (backflow phase), valves 1 and 2 are closed and valves 3 and 4 are opened, while an overpressure is in the fermenter, so that the redundant medium from the bottom of the fermenter vessel is led back to the medium reservoir. During the process, excess gas vents out to the atmosphere through valve 4. Finally, in phase III (resting phase), all valves are closed, and the roots get the opportunity for nutrition uptake under normal atmospheric pressure.

The main challenge in the regulation is to adjust the system so that the optimal medium volume will be sprayed per cycle and the excess medium will be carried back almost completely by the overpressure to the medium reservoir. Furthermore, the pressure should not become too high, to avoid damage in the system and stress to the roots. In the previous function tests, we defined the possible spray volume range by time and backpressure and set the following parameters by the three timers of the central processing unit. For a spray volume of 20 ml, we fixed a spray time of 3.5 sec. In this 3.5 sec, the system pressure rises up to 0.3 bars. This was enough backpressure to lead back the redundant medium to the reservoir (phase II takes 16 sec). The whole system was laid out to stand a pressure of max. 1 bar, but we restricted the max. pressure at 0.5 bars by a pneumatic overpressure valve on the

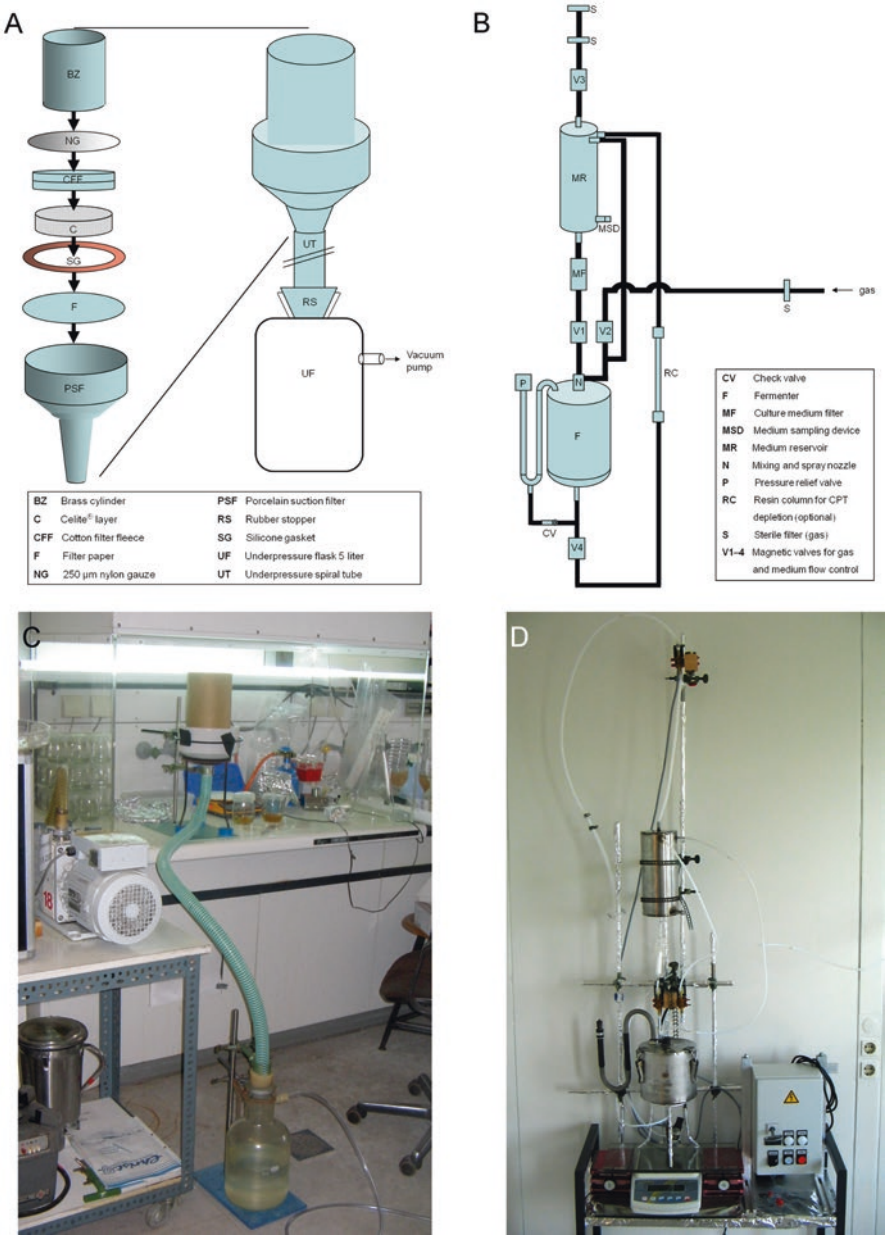

Fig. 6 Schematic and real assembly of the root carrier preparation device (**a**, **c**) and the test mist fermenter WEWA I (**b**, **d**)

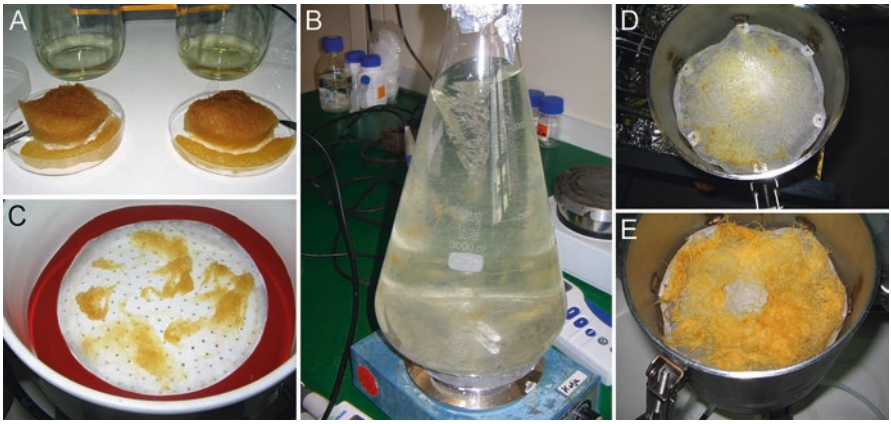

Fig. 7 (**a**) Harvest of untransformed root organ culture tips of *Ophiorrhiza mungos*; (**b**) Dispersion of the inoculum by stirring; (**c**) Agglomerated inoculum on nylon gauze carrier at the beginning of the dispersion tests; (**d**) 4 g inoculum nearly equally dispersed on nylon gauze carrier fixed in fermenter; (**e**) 25.5 g inoculum of transformed root tips (line 607) after 44 h of fermentation with central spray gap

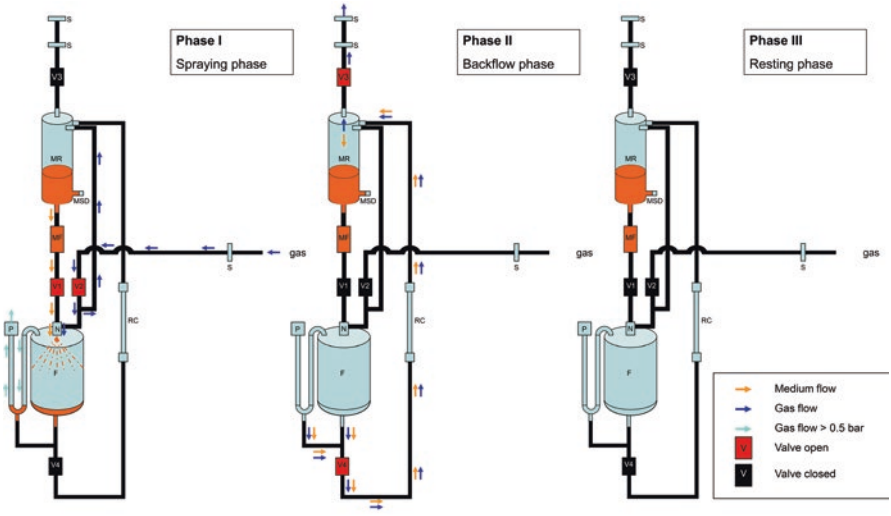

Fig. 8 Functional scheme of the WEWA I with the three-phase cycle. Abbreviations see Fig. 6b

fermenter vessel (Figs. 6b and 8). The medium volume of 20°ml was enough to ensure a good medium exchange in the root inoculum, especially in relation to the interstitial capacity of the roots. Root cultures were able to store up to three times more medium in relation to their own weight. One cycle takes at least 15 min, including the resting phase.

Finally, the problem of sterility was important, on the one hand fundamentally and on the other hand with regard to sample-taking. As mentioned, bacteriostatic and fungicidal substances were added to the culture medium, because it was nearly impossible to get the whole system totally sterile by autoclaving and other kinds of sterilization with our available facilities. Especially the integration of the fermenter vessel with the inoculum and the fixture of the sterile valves were critical points. Also, the sampling of the medium has to be considered under the aspects of sterility and pressure. Therefore, a special medium sampling device was integrated into the medium reservoir (Figs. 6b and 8), so that it was possible to take medium samples by sterile syringes during fermentation.

In this section, the first results of a fermentation of transformed root tips (line 607, 25.5 ± 0.5 g inoculum) over 19 days (with a CPT depletion trail by a XAD PAD II resin column between day 12 and 13) and a fermentation of untransformed root tips (25.7 ± 0.5 g inoculum) over 22 days with a culture medium exchange at day 10 are illustrated.

3 Results

3.1 Basic Morphological and Histological Studies of Ophiorrhiza mungos

Ophiorrhiza mungos is a crude perennial tropical dicotyledonous plant (Fig. 9a). The cross section of the stem axis showed in the centre a more or less unstructured parenchymatous pith surrounded by the typically mostly closed xylem cylinder of the Rubiaceae (Figs. 10a, c and 11a, b). Further outwards, the related phloem elements follow in regular intervals and create open collateral bundles (Fig. 10b–d). After a cortical parenchyma, on average eight to nine cell layers thick, and a four cell-layer thick angular collenchyma, an epidermal monolayer with wax coating formed the final tissue. The first three cell layers of the cortical parenchyma next to the phloem contain crystal granular bodies, as well as raphides and scattered druses, most likely consisting of kinds of oxalate.

The leaves showed the anatomy of a dicotyledonous, zygomorphic, bifacial leaf with upper and lower monolayer epidermis with cuticle, palisade parenchyma, and spongy parenchyma. The stomata were localized on the abaxial leaf surface (e.g. Fig. 2q). The thickness of 300 to 400 μm of the leaves was quite low.

The stem and leaves were covered with unevenly distributed hairs. Here, two types of hairs were present. The first type consists of two cells, a basal one and a second pointed one (Fig. 12c, g). The second type was multicellular, with an additional basal cell (Figs. 10b and 12e, f).

The structure of the inflorescence looks similar to a corymbose cyme, mostly with 7–11, sometimes more, branches (Fig. 9b). The flowering sequence takes place from the centre to the outside. Flower buds, flowers, and seed capsules have stalks.

The seeds of *O. mungos* are minute (1 gram of *O. mungos* seeds contains approx. 60,000 single seeds of angled habitus, Fig. 9c). The whole surface of the inflorescences was covered with a third type of hairs, which only exists there. They seem to be glandular hairs, because the surface becomes sticky when touched. They look like little strawberries, because of a partly thinner cuticle. For that, we named them 'strawberry hairs' (Fig. 11f).

The plant root of *O. mungos* showed homorhizy, even though it is a dicotyledonous plant. The young plant root showed a longitudinal habitus and the root of an old plant a spherical one (Fig. 9a down right). The branching factor was mainly of the second, rarely of the third, order. Morphologically, the plant root showed the typical anatomy of a plant root with stele and cortex without any special modifications.

Fig. 9 (**a**) Flowering, adult plants of *Ophiorrhiza mungos* in the greenhouse and one of their homorhizous, spherical roots; (**b**) Single inflorescence of *O. mungos* (reprinted from Wetterauer et al. (2018), Copyright (2018) Springer Nature Singapore, with permission from Springer); (**c**) Comparison of the seed sizes between *Camptotheca acuminata* (on the left) and *O. mungos* (on the right)

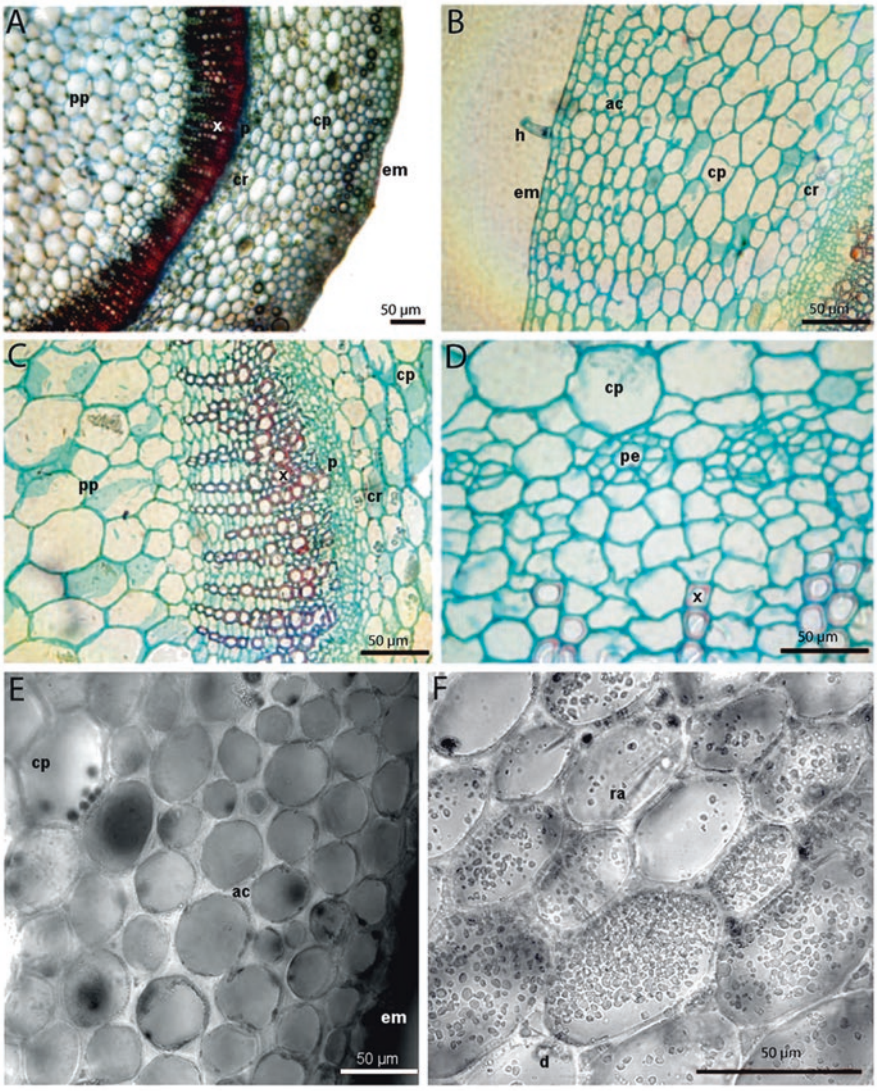

Fig. 10 **a**–**d**: Histological images of a cross section of the stem axis of *Ophiorrhiza mungos* with safranin-fast green stain taken by light microscopy: (**a**) Overview of the cross section of the stem axis; (**b**) Hair, epidermal monolayer, angular collenchymas, and cortical parenchyma; (**c**) Vascular cylinder with adjacent parenchymatous pith and cortical parenchyma; (**d**) Region of cambium with phloem elements of the open collateral bundles. **e** + **f**: Transillumination images of the stem axis of *O. mungos* in situ taken by confocal laser scanning microscopy: (**e**) Angular collenchymas; (**f**) Crystal layer with raphides, druses, and crystal granulous bodies. *ac* angular collenchymas, *cg* crystal granulous bodies, *cp* cortical parenchyma, *cr* crystal layer, *d* druses, *em* epidermal monolayer, *h* hair, *p* phloem, *pe* phloem element, *pp* parenchymatous pith, *ra* raphides, *x* xylem (red)

3.2 *CPT Localization in the Aerial Parts of* Ophiorrhiza mungos

In the aerial parts of *O. mungos*, the storage of CPTs takes place in the vacuoles of idioblastic storage cells. In the stem axis and the side shoots, these storage cells were evenly distributed in the angular collenchyma. The epidermis and the parenchymatous pith did not contain CPT storage cells (Figs. 2k–o and 11b, d, e).

In the leaves, single CPT storage cells or groups of them appeared in the upper and lower epidermis (Figs. 2p–t and 12a, b, d). The spongy and the palisade parenchyma were CPT-free. The leaf stalks showed evenly distributed CPT storage cells in the parenchyma (Fig. 12d).

Additionally, most of the stem and leaf hairs of the two cell types contained CPTs in their vacuoles too (Fig. 12c, g). If the multicellular type contained CPT, it was localized in the cytosol (Fig. 12e, f).

The inflorescences of *O. mungos* showed a high content of 9-methoxy CPT (cf. Figs. 19 and 20). We could thus detect high fluorescence in the receptacles and the flower buds. However, we were not able to differentiate the subcellular localization of CPTs in those parts, because of the high fluorescence of all compartments. Only the ovules seemed to be CPT-free (Fig. 12h, i).

3.3 *CPT Localization in the Plant Root and Transformed as well as Untransformed Root Organ Cultures*

In all studied roots, only pure CPT could be detected, but no derivatives. In principle, the cortex and the stele were CPT-free and the CPT was localized in the border tissues. The cellular and subcellular localization of the CPT in the plant root and the transformed and untransformed root organ cultures differs in the calyptra, the exodermis, and the rhizodermis, as shown in the scheme of Fig. 13.

In the plant root, we were able to detect CPT in the rhizodermis between the root-hair zone and the calyptra localized vacuolarly. The calyptra was CPT-free in principle (Figs. 13 and 14c–e). In the rhizodermis of the root-hair zone and the exodermis of the elderly root parts, the subcellular compartmentation of CPT was vacuolar as well as cytosolic (Figs. 2f–j, 13 and 15f–i).

In untransformed and transformed root organ cultures, the occurrence of CPT in the exodermis of the elderly root parts was strictly vacuolar (Figs. 13 and 15d). In the region of elongation and the zone of differentiation in both root types, the CPT was localized in the cytosol (Figs. 13, 14a, b and 15a, c). In the calyptra of both root

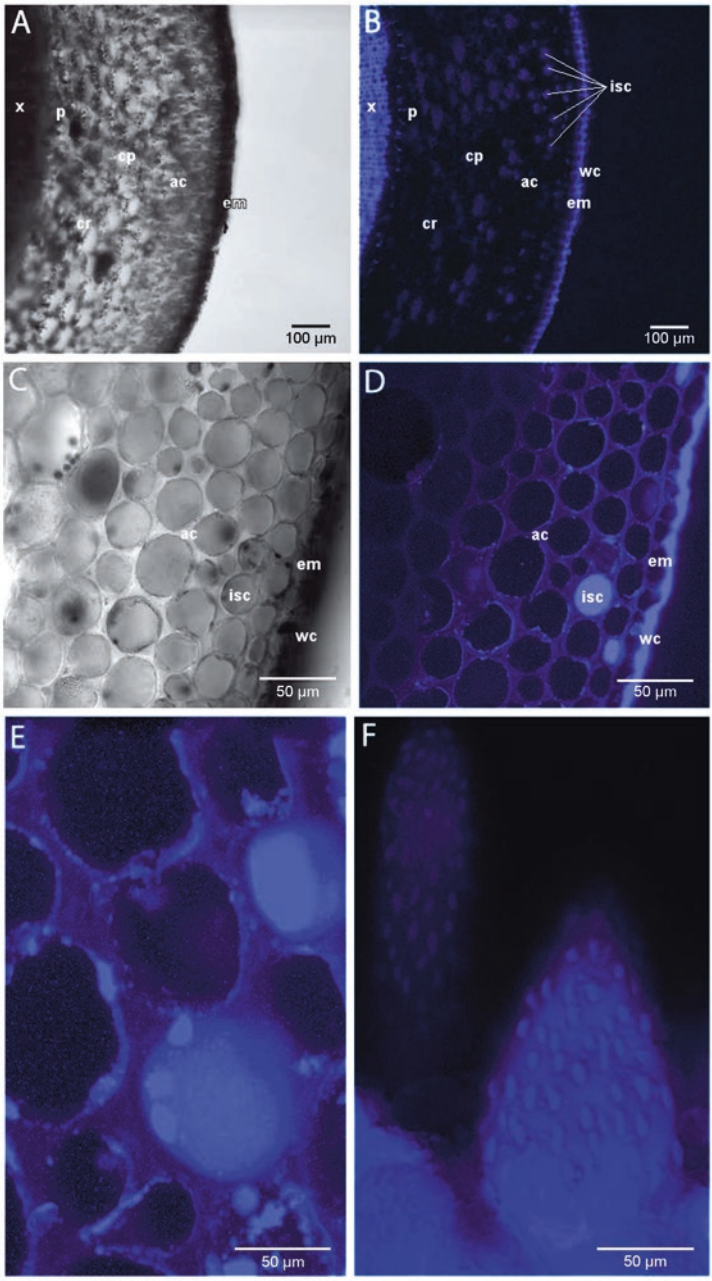

Fig. 11 Transillumination and fluorescence images in situ taken by confocal laser scanning microscopy. **a**–**e**: Selected cross section of the stem axis of *Ophiorrhiza mungos*. (**a**) Overview of stem axis cross section, transillumination image; (**b**) Overview of stem axis cross section (like A), fluorescence image at 405 nm excitation wavelength; (**c**) Selected section image of the angular

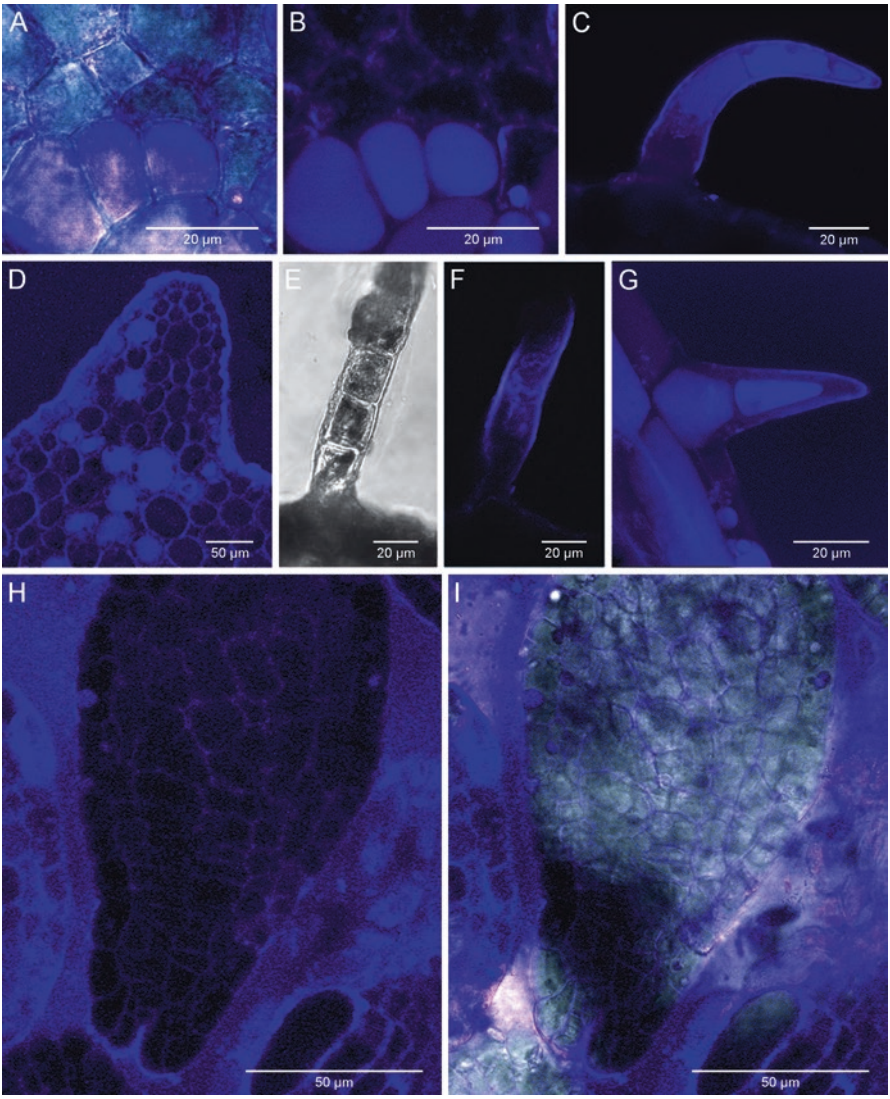

Fig. 12 Transillumination and fluorescence (405 nm excitation wavelength and 470 nm emission wavelength) images and overlays of both in situ taken by confocal laser scanning microscopy of *Ophiorrhiza mungos*. **a** + **b**: Overlay image (**a**) and fluorescence image (**b**) of a group of idioblastic storage cells of the adaxial leaf epidermis; **c**, **e**, **f**, **g**: Two- and multicellular hairs with basic cells of the leaf and stem surface with and without vacuolar CPT storage; (**d**) Leaf stalk parenchyma with evenly distributed CPT storage cells; **h** + **i**: Fluorescence image (**h**) and overlay image (**i**) of CPT-free ovule

Fig. 11 (continued) collenchymas and the epidermis of the stem axis cross section, transillumination image; (**d**) Selected section image of the angular collenchymas and the epidermis of the stem axis cross section (like C) with fluorescent vacuoles in the idioblastic storage cells and fluorescent epidermal wax coating, fluorescence image; (**e**) Reconstructed 3D fluorescence image from a z-stack of CPT containing vacuoles of the idioblastic storage cells in the angular collenchymas of the stem axis cross section; (**f**) Glandular hairs (named 'strawberry hair') of the inflorescence regions of *O. mungos* in situ, fluorescence image at 405 nm excitation wavelength. *ac* angular collenchymas, *cp* cortical parenchyma, *cr* crystal layer, *d* druses, *em* epidermal monolayer, *isc* idioblastic storage cells, *p* phloem, *wc* epidermal wax coating, *x* xylem

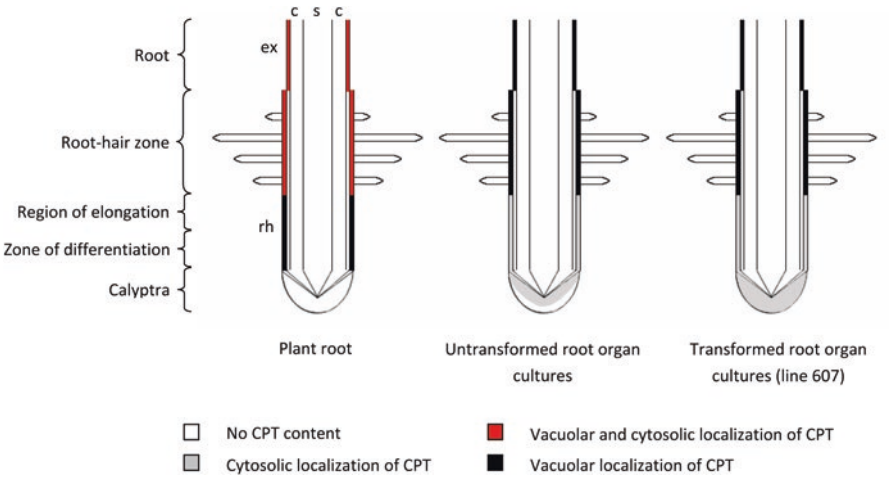

Fig. 13 Comparative scheme of CPT localization on the cellular and subcellular level in root tips of the plant, as well as untransformed and transformed root organ cultures of *Ophiorrhiza mungos*. *c* cortex, *ex* exodermis, *rh* rhizodermis, *s* stele

culture lines, a cytosolic localization was observed. But in the untransformed roots, the front part of the calyptra was generally CPT-free (Figs. 13 and 14a). On the other hand, the transformed roots showed cytosolic CPT storage in all parts of the calyptra (Figs. 13, 14b and 15a, b). This general scheme of localization is not absolute and can vary a little in the individual roots, especially in the rhizodermis and calyptra of the root organ cultures.

The root hairs seem in general to contain no CPT (Fig. 15e). Sometimes, there is the appearance of a slightly cytosolic condition of CPT in some root hairs, but we were not able to confirm this.

3.4 CPT in Root Exudates of Transformed Root Organ Cultures

To our surprise, we could not detect any CPT in the liquid phase of the harvested root exudates. Instead, we found fluorescent crystals in the root exudates by fluorescence microscopy (Fig. 16a). No quantitative studies could thus be performed here. Based on the histological studies of the cross section of the stem axis (Fig. 10f), we proposed that these crystals probably consist of calcium oxalate with embedded CPT. In order to verify this hypothesis, a precipitation of calcium oxalate in a

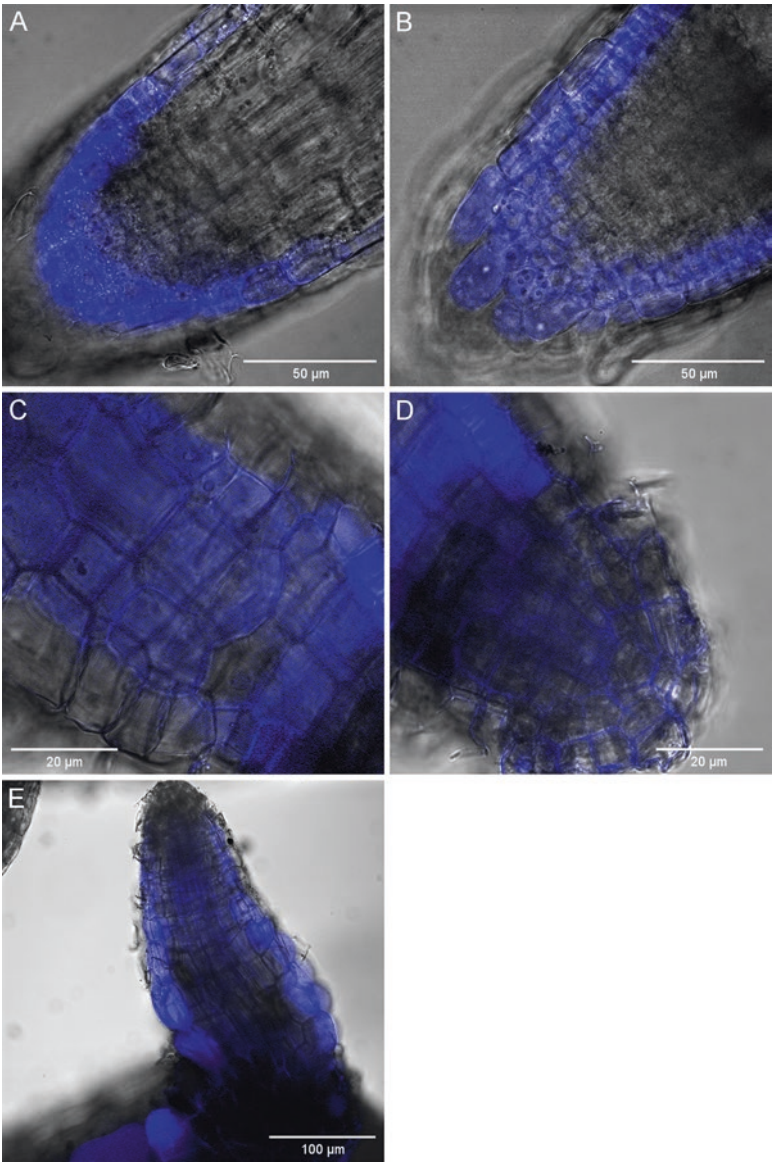

Fig. 14 CPT distribution in root tips in plant root and root organ cultures in situ of *Ophiorrhiza mungos*. Combined fluorescence and transillumination images taken by confocal laser scanning microscopy (405 nm excitation wavelength and 470 nm emission wavelength). (**a**) Root tip of untransformed root organ culture; (**b**) Root tip of transformed root organ culture (line 607); (**c**) + (**d**) Root tip of plant root [zone of elongation and differentiation (**c**), calyptra (**d**)]; (**e**) Young lateral root of plant root

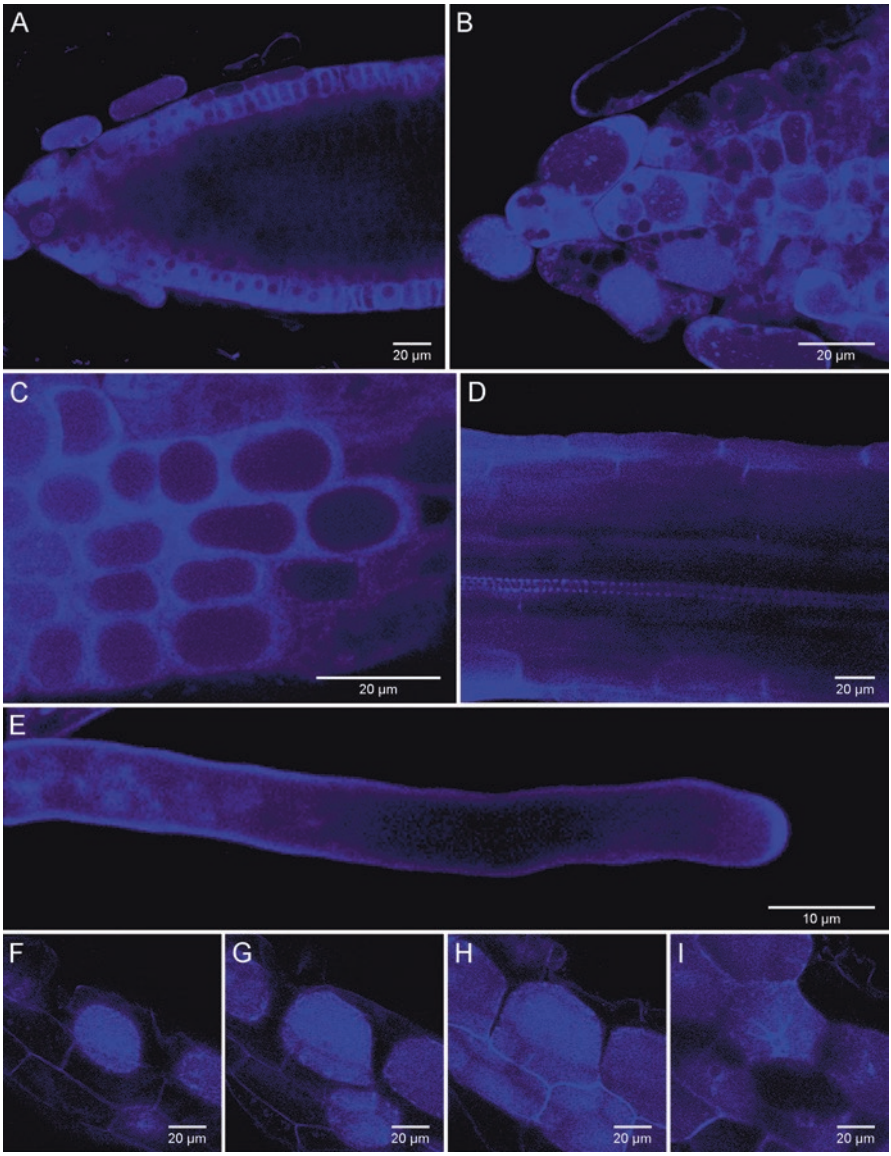

Fig. 15 Fluorescence images in situ taken by confocal laser scanning microscopy (405 nm excitation wavelength and 470 nm emission wavelength) of selected regions of transformed root organ cultures (line 607) of *Ophiorrhiza mungos*. **a–e**: (**a**) Overview of longitudinal section of root tip; (**b**) Calyptra; (**c**) Rhizodermis in the region of elongation; (**d**) Longitudinal section in the old root with exodermis and xylem elements of the stele; (**e**) Growing root hair; **f–i**: Vacuolar and cytosolic CPT fluorescence in situ in the rhizodermis of the plant root of *O. mungos*: (**f**) Cut vacuoles; (**g**) Central layer through vacuoles; (**h**) Surface of the rhizodermis; (**i**) Cytosolic fluorescence and nucleus in negative contrast

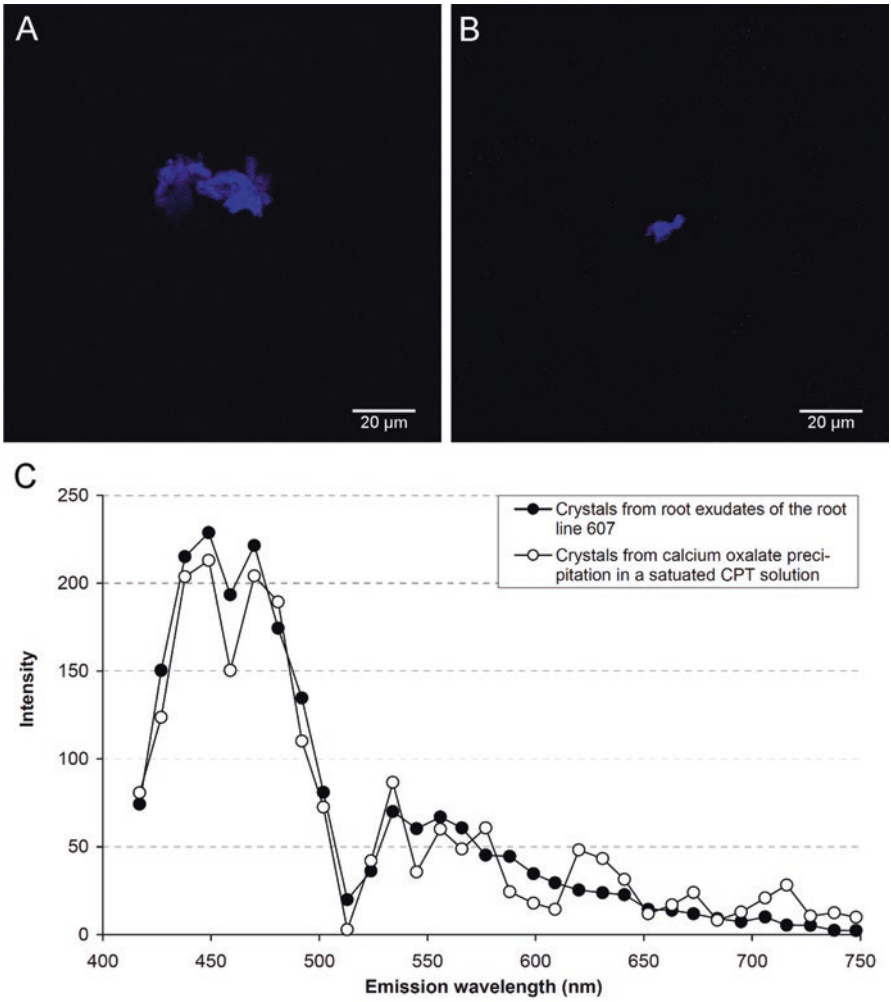

Fig. 16 Confocal laser scanning microscopy images of root exudate crystals of the root organ culture line 607 of *Ophiorrhiza mungos* (**a**) and calcium oxalate crystals precipitated in a saturated CPT solution (**b**). (**c**) Lambda scans of crystals of A and B measured by confocal laser scanning microscopy. Excitation wavelength at 405 nm; measurements ensue in 50 mM KH_2PO_4 solution

saturated and filtered CPT solution was executed. After repeatedly cleaning the precipitate, we could detect some fluorescent oxalate crystals (Fig. 16b) and thus verify that CPT can be included in calcium oxalate crystals. A comparison of the fluorescent root exudate crystals with the self-prepared calcium oxalate crystals by lambda scans made this obvious (Fig. 16c). The other calcium oxalate crystals without CPT did not show any fluorescence.

3.5 *CPT Contents and Distribution in Young and Adult Plants of* Ophiorrhiza mungos

In the next step, the qualitative and quantitative distributions of CPTs in the total plant were investigated. To this end, a young 10-week-old *O. mungos* plant clone and an approx. 6-month-old flowering plant were harvested and the contents of CPT and 9-methoxy CPT determined in every plant part.

In the young plant (Figs. 17 and 18), the highest relative yields of CPTs were found in the youngest leaves (about 1664 µg/g DW or 304 µg/g FW) with an approx. 60% proportion for 9-methoxy CPT. All other plant parts varied between 400–1000 µg/g DW and 50–150 µg/g FW, respectively, in the relative contents of the CPTs. In this context, the proportion of 9-methoxy CPT was 60–90% in the leaves. The proportional content of CPT increased down the stem axis by up to 50–70% and in the root by up to 99%. The highest absolute CPT yield in the plant was found in the root with 70 µg CPT, which correlated with 52.6% of the complete CPT in the whole plant; the root biomass was about 20% of the total plant. In the stem axis, the absolute CPT content was about 35 µg CPT (26.3%) and in the leaves 28 µg CPT (21.1%). A different picture was shown for 9-methoxy CPT. Here, the root contained only 1 µg (0.4%), the stem axis 18 µg (8.5%), and the leaves 194 µg 9-methoxy CPT (91.1%). The whole young plant contained 106 µg CPTs/g FW and 795 µg CPTs/g DW, or in total 212 µg 9-methoxy CPT and 134°µg CPT (total FW, 3.27 g; total DW, 0.44 g; DW/FW ratio, 13.46%).

In contrast to the young plant, the adult plant of *O. mungos* (Figs. 19 and 20) shows a more complex picture of absolute and relative CPT yields. Basically, again the predominant alkaloid in the aerial parts was 9-methoxy CPT and CPT in the root. The absolute CPT content in the root was about 3163 µg CPT, which correlated with 87.1% of the complete CPT in the whole plant; the root biomass was about 41.3% DW or 29.5% FW of the total plant, respectively. Therefore, the root contained 66% of the total CPTs. The aerial parts (58% of DW or 70.5% of FW) showed a total content of CPTs of 34% 460 µg CPT and 1164 µg 9-methoxy CPT of the whole plant, but contained 94.75% of the total 9-methoxy CPT.

On closer examination of the aerial parts, a reduction of the CPT yields from the roots to the main inflorescence of the stem axis from approx. 500 to 100 µg/g DW became obvious. Inversely, the 9-methoxy CPT content rose in the same concentration range. The young side shoots and their leaves as well as the oldest leaves contained 100–200 µg/g CPT and the other leaves about 0–100 µg CPT/g DW. In the case of 9-methoxy CPT, the leaves contained 200–1500 µg/g DW. The oldest leaves in the lower third showed the highest concentrations of 800–1500 µg/g DW, the leaves of the oldest side shoot contained about 200–800 µg/g DW, the leaves of the next upper node about 400–600 µg/g DW, and the leaves of the supreme node about 200–600 µg/g DW. Therefore, the 9-methoxy CPT tends to decrease in the leaves from bottom up, but on a high level.

The main inflorescence exhibited CPT levels of 100–400 µg/g DW. In this context, the seed capsules were in the lowest range, but showed the highest content of

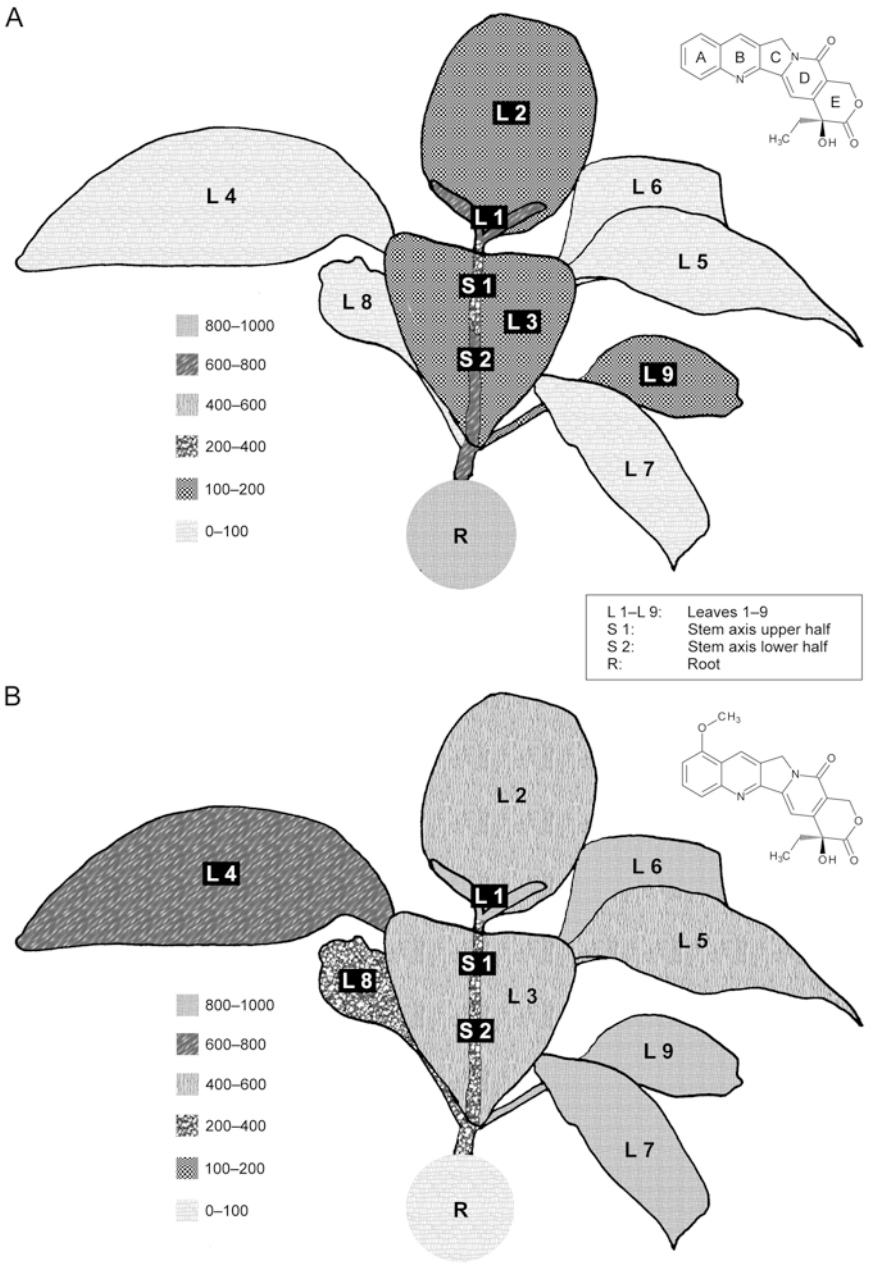

Fig. 17 CPT (**a**) and 9-methoxy CPT (**b**) contents in a young plant clone of *O. mungos* (age about 10 weeks). All values are given in μg/g DW. The graphic representation of the root is simplified and the stem axis has been made visible behind the leaves

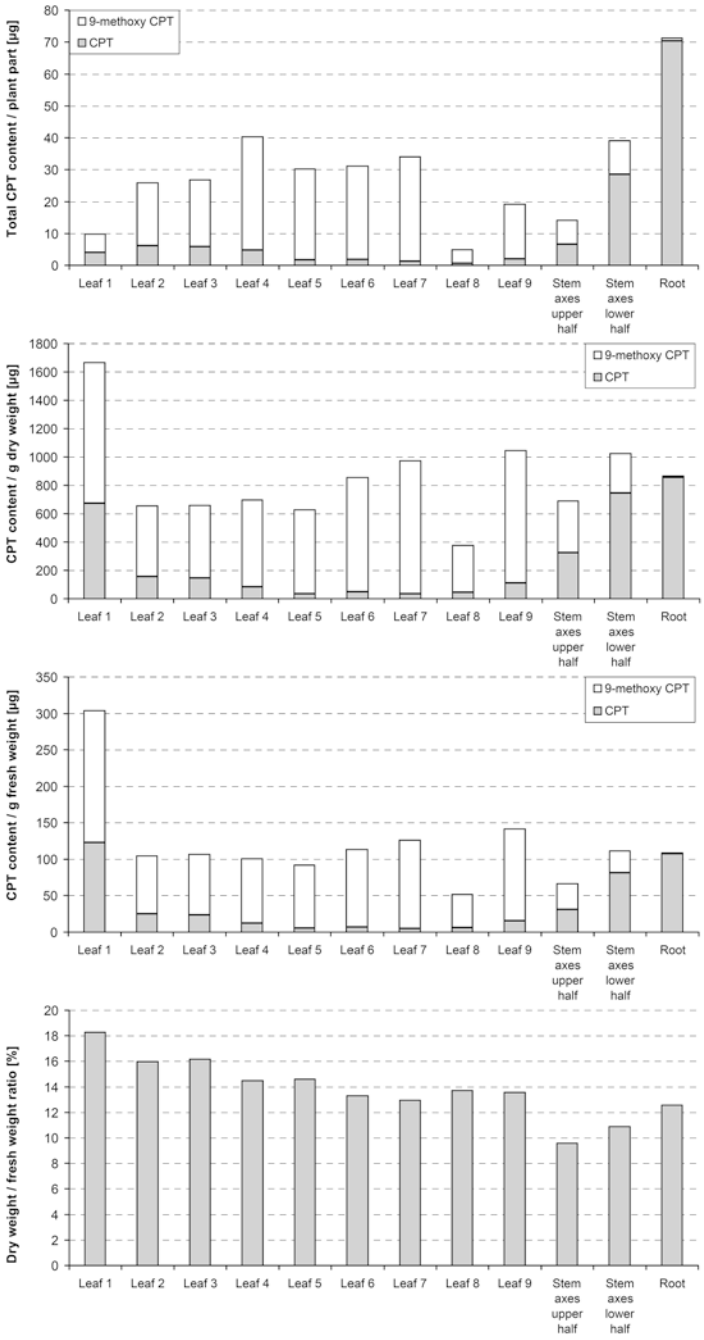

Fig. 18 Contents of CPT and 9-methoxy CPT in different relations and the DW/FW ratio of leaves, stem axis, and root of a plant clone of *Ophiorrhiza mungos* (cf. Fig. 17), about 10 weeks old

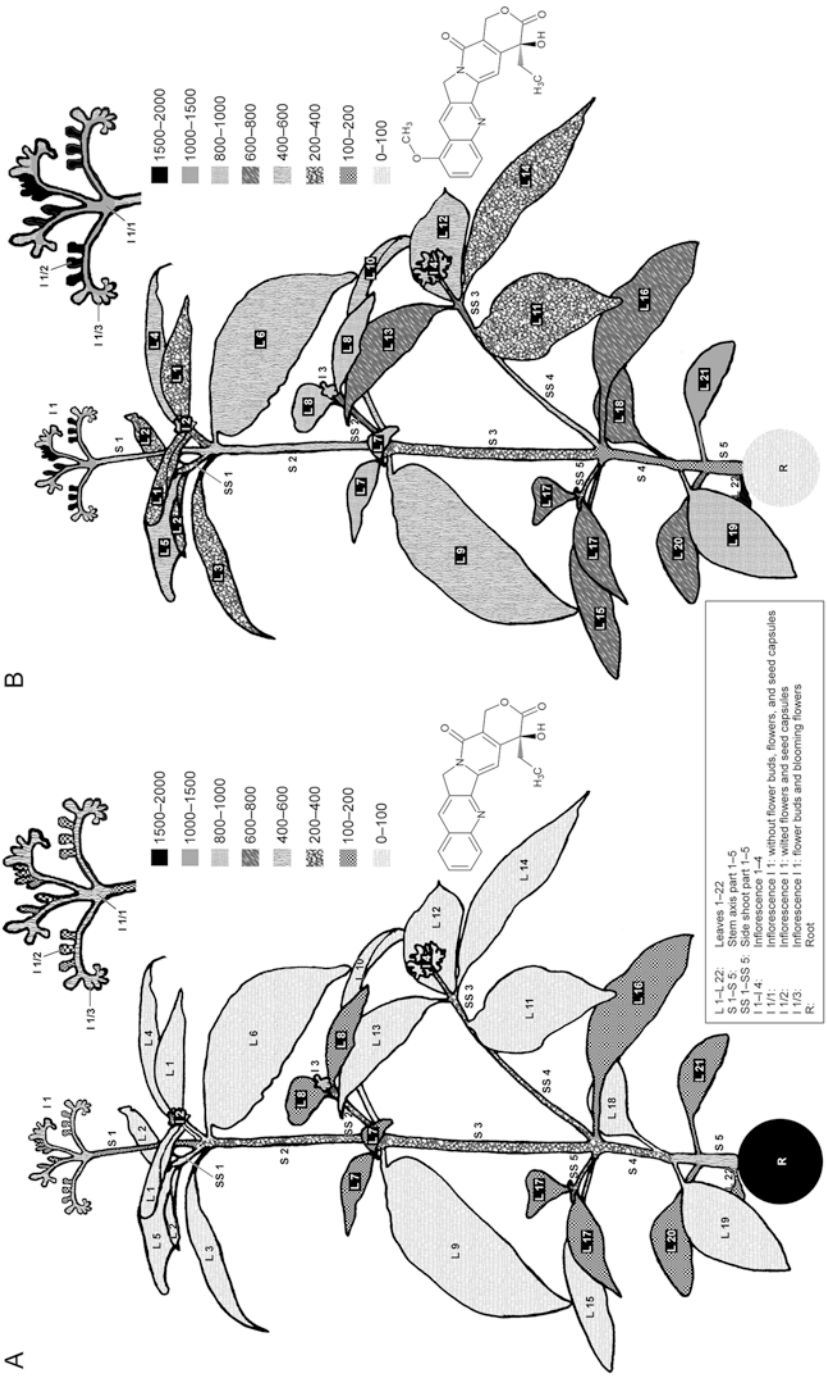

Fig. 19 Contents of CPT (**a**) and 9-methoxy CPT (**b**) in an adult plant of *Ophiorrhiza mungos* (older than half a year). All values are given in µg/g DW. The graphical representation of the root (R) and the main inflorescence (I 1) has been simplified

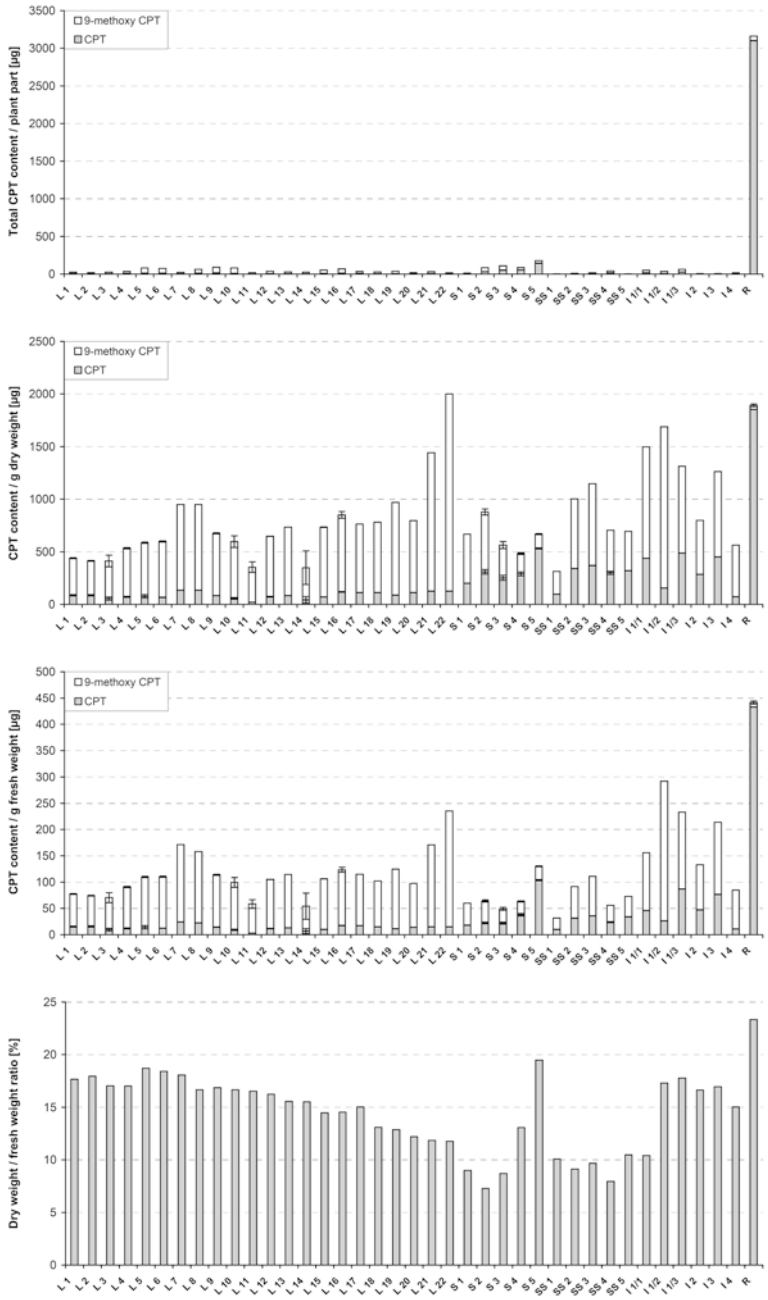

Fig. 20 Contents of CPT and 9-methoxy CPT in different relations and the DW/FW ratio of leaves (L), inflorescence (I), stem axis (S), side shoots (SS), and root (R) of a plant clone of *Ophiorrhiza mungos* (cf. Fig. 19), older than 6 months

9-methoxy CPT of approx. 1800 µg/g DW. The buds and flowers contained about 800–1000 µg/g DW and the rest of the inflorescence between 1000 and 1500 µg/g DW. Consequently, the main inflorescence showed the highest 9-methoxy CPT content and the highest content of CPTs in the aerial parts of the adult plant. In contrast, the minor inflorescences showed a CPT content of 80–450 µg/g DW and a 9-methoxy CPT content of 400–800 µg/g DW.

The whole adult plant contained about 197 µg CPTs/g FW and 1182 µg CPTs/g DW, or in total 1229 µg 9-methoxy CPT and 3559 µg CPT (total FW, 24.29 g; total DW, 4.05 g; DW/FW ratio, 16.68%).

3.6 CPT Distribution Inside Transformed and Untransformed Root Organ Cultures

The CPT content in the root organ tissues is quite stable in relation to FW and DW for each line (cf. Wetterauer et al. 2018). After examination of the distribution and storage of the CPTs in the total plant and the differences in CPT deposition in the plant root in comparison to transformed and untransformed root organ cultures (secs. 3.4 + 3.5), we wanted to know the distribution pattern of CPT in the transformed and untransformed root organ cultures of *O. mungos*. The results are shown in Fig. 21.

Of course, the root parts did not have the same weights because of their different lengths and the manual cutting, but the corresponding parts were in a comparable range. The same was the case in the CPT content per root part. As this implies, the CPT content in both root lines showed the same level for all parts calculated per gram FW; the transformed line is four times less in relation to the untransformed one. The DW to FW ratio rose a little from the younger tissues (part 1) to the older tissues. That means that the younger tissue contains more water than the older ones. In view of this, it is clear that the CPT content per gram DW decreased a little, because the corresponding biomass increased a little. In summary, the CPT content in the total roots of both lines is evenly distributed and related to the primary dry biomass in the oldest parts, because here a swlling of the root exodermis or a secondary growth takes place (browner tissue), or both. The dry weight density emphasizes this change, interestingly by a continuous decrease by age.

3.7 Elicitor Studies

In extensive elicitor studies on *O. mungos* root cultures, we were able to confirm that no amplification of CPT biosynthesis took place by single elicitor treatments. In these studies, many different elicitors, both simple (defined) and complex (defined and undefined), as well as precursors and abiotic stress conditions, were tested (Table 1).

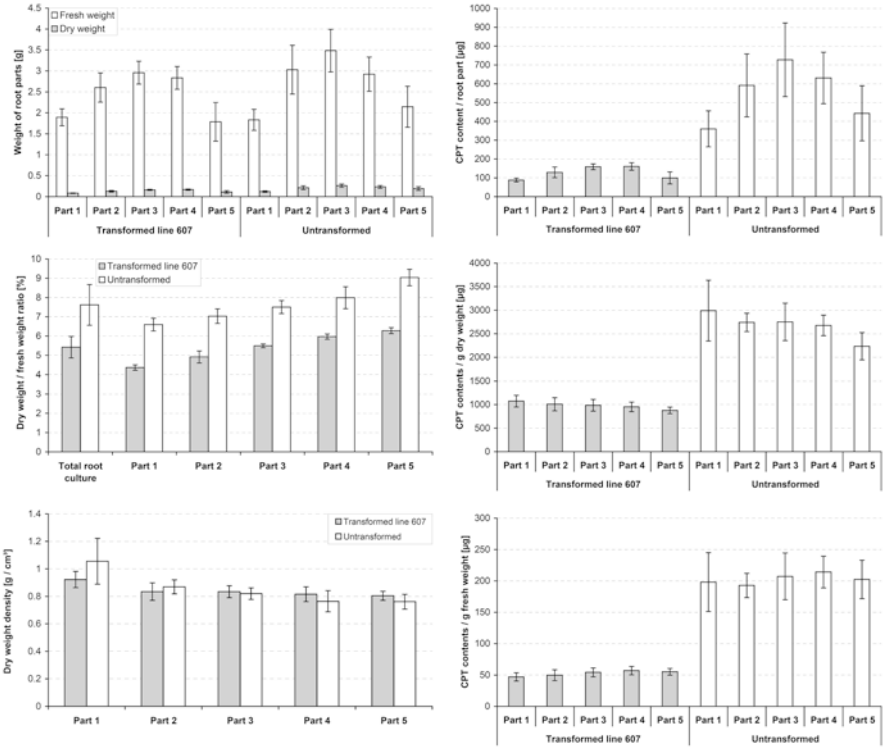

Fig. 21 Weights and CPT content in different relations of 7-week-old transformed and untransformed root organ cultures of *Ophiorrhiza mungos* cut into five parts each (young to old tissue, cf. Fig. 5), as well as their dry weight density (n = 4)

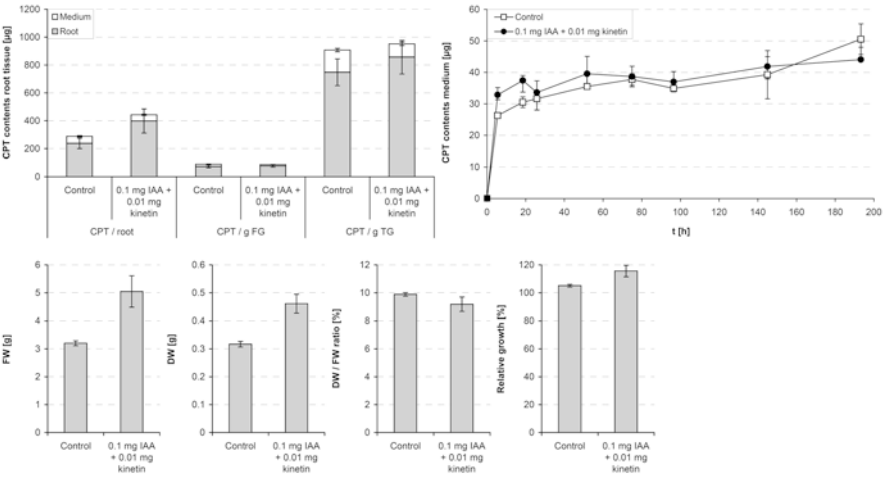

Fig. 22 CPT content in media and root tissues and growth parameters of untransformed root organ cultures of *Ophiorrhiza mungos* by combined treatment with 0.1 mg (≙11.4 µM) IAA and 0.01 mg (≙0.9 µM) kinetin per flask (n = 3)

Only a higher total CPT content, combined with higher relative and absolute growth through indole acetic acid (IAA) and kinetin induction, was detected (Fig. 22). With a higher growth rate, a higher absolute CPT content is realistic, of course. But the relative CPT content in relation to DW did not show the increase in the CPT tissue content as did the absolute ones and in relation to the FW is seen to be even lower in relation to the control. The explanation is quite simple. A brief look at the DW/FW ratio shows that it went down through the hormone treatment. A part of the difference in the absolute growth is based on higher water content in the treated roots. In the end, an increase in CPT tissue content in the treated root tissues can be noticed, but only related to the DW of a higher relative growth rate. This confirms again our hypothesis that CPT biosynthesis seems to be constitutive and growth regulated.

3.8 First Fermentations of Transformed and Untransformed Root Cultures of Ophiorrhiza mungos *in the Test Mist Fermenter WEWA I*

On closer examination of the medium contents during fermentation of the transformed line 607, a good agreement to the course of the corresponding root shaking cultures became obvious (Fig. 23; cf. Wetterauer et al. 2018). As in the root organ cultures, ammonium as a source of nitrogen was preferred, before the nitrate could be taken up. The ammonium content declined in the medium from approx. 0.45 mM to 0.03 mM from 70 to 290 h. In the fermentation time shown, the nitrate was not taken up by the roots and remained at around 15 mM. For longer fermentation, this would be more relevant with regard to growth and the pH value, because during ammonium uptake, the pH became more acidic and during nitrate uptake more alkaline. Here, the pH value became first a little more acidic, up to max pH 5.3 at 216 h during ammonium uptake and afterwards more alkaline nearly pH 6.2 at the end. The reason can be the start of nitrate uptake or other unknown factors. The phosphate content shows nearly the same course as the ammonium content, and the phosphate was taken up nearly completely until the end of the test period at 432 h. The sucrose content went down continuously and was inverted into glucose and fructose in concentrations of max. 1 g/l. At the end of the fermentation period, the sugar was not completely taken up.

The CPT content in the medium rose in the first 48 h up to 0.2 mg/l and increased continuously, at 0.04 mg per day. At the end of the test period, the CPT reached a concentration of 0.7 mg/l (0.2 µM). Only one break during the downstream test by a XAD PAD II column existed at day 13. This test was aborted quickly, because the pressure of the system was too low for the return flow of the medium to the medium reservoir through the column.

During fermentation, the relative growth rate was about 30%, in total 8 g gain. This was relatively low in relation to the root organ cultures, which tripled their fresh weights in the same incubation time. The roots on the carrier show a browning

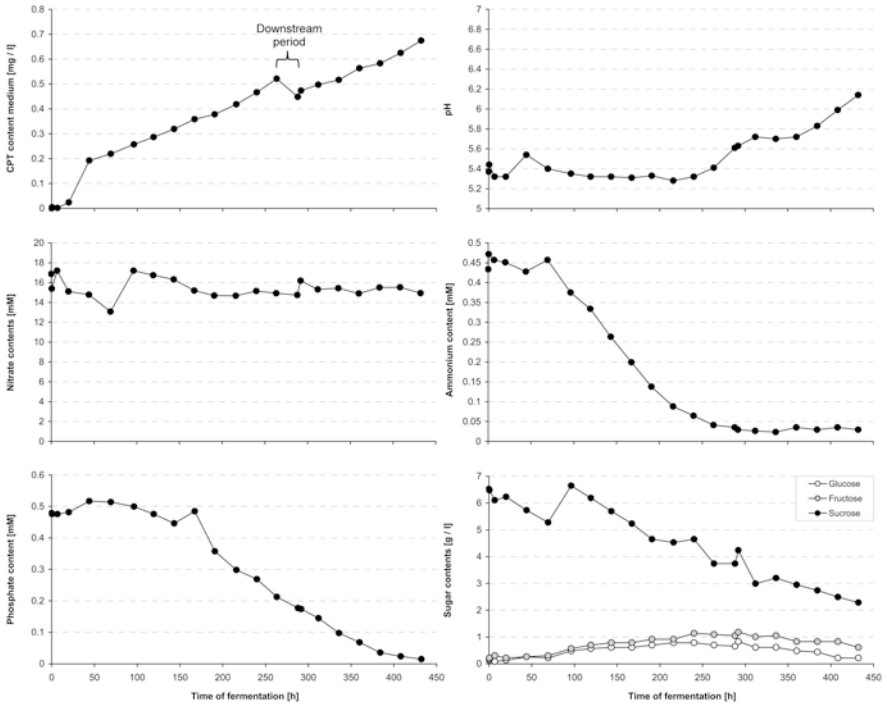

Fig. 23 Medium parameter courses during fermentation of transformed *Ophiorrhiza mungos* root tips (line 607) over 19 days. On day 13, a CPT downstream test by a XAD PAD II column was performed

at the end of the test period (Fig. 24) that implies stress or over-fertilization or both, especially with carbohydrates. In the centre, a spray gap with partially extinct tissue existed (circles in Fig. 24a, b; cf. Fig. 7e). The remaining tissue was vital and robust. Towards the outer half, young root tips were growing on the top and on the bottom side of the carrier. It appears that the medium spray was too strong. To correct this, the distance between the spay nozzle and the root carrier has to be enlarged or the spray pressure has to be reduced by reconstruction of the nozzle or a more indirect spraying method has to be developed for less irritation of the root tissue.

In another fermentation run with untransformed root tips of *O. mungos* over 22 days, a culture medium exchange was conducted after 10 days. In Fig. 25, the CPT medium content, the fermenter vessel weights, and the pH values over the test period are shown. This time, to obtain a better view of the roots' growing behaviour, the fermenter vessel was disconnected briefly at every reading point, and the acquisitions of the root weight course were done by weighing the complete fermenter vessel.

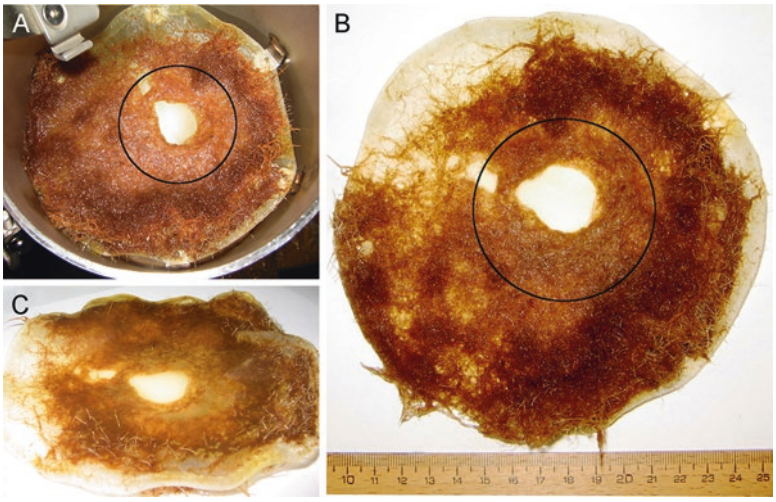

Fig. 24 Root carrier with transformed root tips of *Ophiorrhiza mungos* (line 607) after 19 days of incubation in the test mist fermenter WEWA I. (**a**) Opened fermenter vessel; (**b**) Top side of the carrier; (**c**) Bottom side of the carrier; Circles: central spray gap with partially extinct tissue

The CPT content increased in the first 2 days up to nearly 0.6 mg/l (1.7 µM). This was three times higher than in our experiments with the transformed line and showed the same difference in the medium content between the transformed and untransformed lines as in the root organ cultures (cf. Wetterauer et al. 2018 Fig. 14.5). Afterwards, the CPT content continued to rise up to nearly 0.9 mg/l (2.6 µM), parallel to the root growth, until the medium exchange. Afterwards, the CPT increased in the first 2 days up to 0.3 mg/l and afterwards by about 0.1 mg/l every 3 days. Unfortunately, a bacterial contamination occurred on day 32 (Fig. 25, grey area). Thus, no concrete statements about final CPT contents and absolute and relative growth without bacterial contamination can be given. The growth rate of the untransformed roots seemed to be in the same range as that of the transformed ones. The pH values showed also nearly the same course, until the bacterial contamination. During the contamination, the CPT contents continued to rise without reaching a plateau. The growth data are semi-quantitative and the pH values became more and more alkaline.

In summary:

For improvement, a longer period of optimization of the culture conditions and technical changes are necessary. Also, more effort has to be put to the sterile handling. But, in principle, a CPT fermentation of roots of *O. mungos* is feasible. Additionally, continuous or interval downstream processing for CPT out of the culture medium has to be developed.

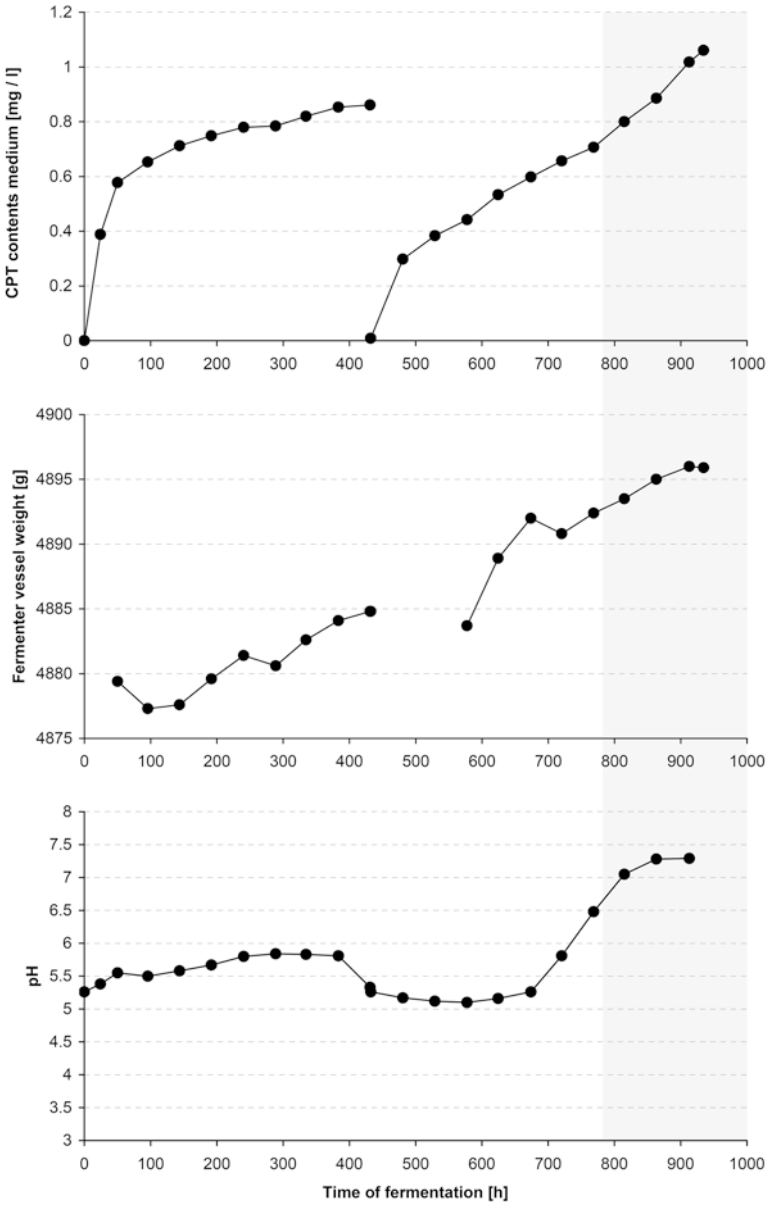

Fig. 25 CPT content, pH values, and approx. fermenter vessel weight during fermentation of untransformed root tips over 22 days. At day 10, a culture medium exchange was conducted

4 Discussion

Initially, only places of findings, basic morphological descriptions, and the traditional usages of *O. mungos* existed in the available literature (i.a. Hooker 1882; Kirtikar and Basu 1975; Nadkarni 1927; Quisumbing 1978; Sanyal 1984; Thwaites 1864; von Linne' 1753). The rest of the literature covered phylogenetic aspects of the Rubiaceae. Even nowadays, the genus *Ophiorrhiza* has not been thoroughly analysed. This becomes obvious when looking at the number of species, a number varying from 50 (Li and Adair 1994) up to 150 (Beegum et al. 2007; Darwin 1976). Additionally, this genus is problematic owing to double or multiple species descriptions, and thus synonyms are common (cf. nomenclature database of the Botanical Garden of Missouri).

Interestingly, Darwin (1976) discussed, besides other taxonomic characters, the occurrence or absence of crystals and raphides in *Ophiorrhiza* species as a marker for the position within the Rubiaceae system. However, the crystals were not a continuously present character either in the different *Ophiorrhiza* species or in the studied tissues. In addition, exactly *O. mungos* was not part of the species considered. In the present study, we describe the occurrence of crystals (raphides, druses, and crystal granular bodies) in this plant for the first time, at least in the border region of the cortical parenchyma near the phloem of the stem axis (cf. Fig. 10, Wetterauer 2008). Later, we will hypothesize why these crystals can be found there. At first, other parts of the plant were not investigated in relation to the occurrence of crystals, because we placed the main focus on the CPT distribution. But we were able to determine indirectly, by our studies of the root tip exudates of the root organ cultures (q.v. Flores et al. 1999), that the crystals consist of calcium oxalate (cf. Fig. 16). Afterwards, we prepared some handmade sections of *O. mungos* leaves and were able to detect microscopically that needles are present in the leaves (data not shown). In all the investigated root tissues, crystals, in whatever form, were never observed. Some years ago, Madhavan et al. (2013) did a pharmacognostical study on the leaves of *O. mungos*, but they did not describe any crystals or needles in the investigated tissues apart from the macerated trichomes. We can confirm a granulose appearance within the trichomes, but during our confocal laser scanning microscopy studies, we were not able to detect any real crystals in the living trichomes (Fig. 12c + E–G). However, the presence of calcium oxalate was verified by the histochemical tests of Madhavan et al. (2013).

All of our further findings in relation to the morphology of *O. mungos* were in agreement with the existing literature, apart from one new discovery. We were able to detect for the first time a new type of glandular hair on the surface of the inflorescence of *O. mungos*. We have called them 'strawberry hairs' because of their appearance (cf. sec. 3.1 + Fig. 11f).

When focussing on the CPT content and other ingredients in *O. mungos*, the historical view is quite interesting. Nadkarni (1927) first described that *O. mungos* contains an amorphous alkaloid (the method of detection was not given) besides starch, resin, and fat. Agarwal and Dhar (1959) isolated β-sitosterol and two

ergosterol derivatives out of the roots, and Tafur et al. (1976) determined for the first time CPT (12 μg/g DW) and 10-methoxy CPT (10.4 μg/g DW) in the leaves of *O. mungos*. In contrast, Sanyal (1984) remarked that no alkaloids were detected in *O. mungos*, but starch, chlorophyll, and a light-brown resin soluble in chloroform. In 2005, we published for the first time the CPT concentrations in our transformed and untransformed root organ shaking cultures of *O. mungos* (890–3200 μg/g DW, Wink et al. 2005), and Roja (2006) gave CPT concentrations for plant roots (176 μg/g DW) and shoots (96 μg/g DW) and for 9-methoxy CPT (only traces in both). Therefore, the question occurs why the content of CPTs in *O. mungos*, as determined by Tafur et al. and Roja in plants from natural habitats, should be so low in relation to the content levels in our data from root cultures or the concentrations in the plant roots with 860–1850 μg CPT/g DW and the aerial parts with 179–193 μg CPT/g DW and 490–600 μg 9-methoxy CPT/g DW, or total CPT contents with 795–1182 μg/g DW. First, we had a suspicion that the common method of defatting with petroleum ether may be a factor. In this regard, we tested the defatting of herb material with petroleum ether, followed by our normal extraction procedure, and saw no differences in the contents of CPTs. A degradation of the very stable CPTs by common handling of the drug is nearly impossible. Thus, we assume that the plant material of *O. mungos* from the natural sources in comparison to our greenhouse plants, or other factors of the declared methods, may be responsible for the low concentrations of CPTs given in these publications. Renjith et al. (2013, 2016) extracted the entire plants of *O. mungos* from a total of 17 different collection locations and obtained CPT contents between 150 and 540 μg CPT/g DW, but unfortunately analyses of other CPT derivatives were not described. We determined 300–880 μg CPT/g DW in our plants in total and of this 52.6–87.1% was localized in the roots. This confirms our hypotheses, because, on the one hand, Renjith et al. had lower CPT values, but in the same range. That indicates a slightly lower content in natural collected plant material (cf. Pasqua et al. 2004). On the other hand, even if the natural plant material has lower CPT values, the really low CPT and 9-/10-methoxy CPT values in Tafur et al. and Roja can only be explained by a big loss during the extraction procedure or a not fully developed quantitative analytic method. Next, Deepthi and Satheeshkumar (2016, 2017a, b) published studies on cell suspension and adventitious root cultures and Nagesha et al. (2018) on in vitro cultures of *O. mungos*; we will discuss these later in comparison to our elicitor studies. Finally, we gave an overview of nearly all published CPT content data in plants, a comprehensive look at the CPT content of 1 untransformed and 23 transformed root organ culture lines of *O. mungos*, a comparison of their culturing behaviour, and an overview of the CPT content in different plant tissues and cell culture systems of *O. mungos* (Wetterauer et al. 2018).

We mainly focussed on the distribution and storage of the CPTs within the tissues of the plant and the transformed and untransformed root organ cultures of *O. mungos*, especially in relation to the ecological function of CPTs as defence chemicals. At the time, nothing was known about CPT or its function; the usage in the traditional medicines gave first hints. First of all, the bitterness of the drug was described (Kirtikar and Basu 1975; Nadkarni 1927; Quisumbing 1978; Sanyal 1984), very probably due to the CPTs. Leaves, roots, and bark were used in the

forms of decoction, paste, or pressed juice (out of fresh roots, stem, and leaves), as described in the literature just mentioned. Looking in more detail at the parts of *O. mungos* used as a drug, we observed that these correspond to the localization of the CPTs we found in our in situ confocal laser scanning microscopy studies (cf. secs. 3.2 + 3.3). In general, the CPTs can be detected in the outer tissues of *O. mungos*. The highest concentrations are included in the most sensitive tissues as young leaves of young plants or the main inflorescence. This parallels the findings of Yamazaki et al. (2003b) in *O. pumila* or of López-Meyer et al. (1994) in *C. acuminata*. In *O. mungos*, CPT was stored vacuolarly and cytosolically in the root dermata. In the aerial parts, the CPTs are localized vacuolarly in evenly distributed idioblastic storage cells of the outer parenchymatic tissues, in the epidermis of the abaxial and adaxial leaf surface, and in the surface hairs of the two- and multicellular type (cf. Shitan and Yazaki 2007). Thus, a classical protection and defence pattern against herbivores becomes obvious in all parts of the plant (e.g. De Luca and St Pierre 2000; Wink 1988, 2003). The parenchymatous piths and epidermis of the stem axis and side shoots, the spongy and palisade parenchyma of the leaves, the vascular bundles, and the ovules as well as the calyptras of the root and the root hairs were free of CPTs.

Very interesting are the differences in localization and storage of CPT of the plant root and the transformed and untransformed root organ cultures besides one common aspect, that the stele and the cortex of all of them were CPT-free (Figs. 13, 14, and 15a–d, f–i). In the plant root, the calyptras are CPT-free and the storage is vacuolar in the rhizodermis, initial from the zone of differentiation. With the beginning of the root-hair zone, in addition a cytosolic storage can be noticed upwards. In contrast to the plant root, the untransformed root organ cultures show a cytosolic localization starting in the middle of the calyptras and go up in the cone to the rhizodermis. In the root-hair zone, the storage switches to a vacuolar one. Finally, the root organ cultures of the transformed line 607 showed the same storage and localization as the untransformed ones, with one difference that the calyptras show in total a cytosolic CPT fluorescence (comp. Fig. 13). Why the storage is different belongs to the field of speculation at the moment and needs to be investigated more closely. Maybe the big differences in storage and distribution of CPT between the plant root and the root organ cultures can be attributed to another mode of auxin metabolism, because of the non-existent aerial parts. But here, many further questions will come up in relation to CPT biosynthesis, vacuolar storage, transport, self-protection against the plant's own CPT, and the release in the surrounding medium, as well as its content regulation there, which will be discussed below.

The CPT in the roots and root organ cultures of *O. mungos* is localized in the border tissues, beginning with the zone of differentiation. Apart from the different modes of location and storage in the transformed and untransformed root organ cultures, the CPT appears also in the calyptras, first within the differentiated tissues or the tissues that are in the process of differentiation. Next, the distribution of the CPT within the root organ cultures is equal in relation to the dry biomass. That means all root sections contain the same relative CPT content (cf. sec. 3.6). This

suggests, together with the absolute stable CPT contents in our root organ lines and the clear vacuolar storage of CPTs in the evenly distributed cells of the aerial parts, a developmentally regulated CPT biosynthesis for a constitutive purpose. In a study by Asano et al. (2004), three plant species (aseptic culture) were investigated, and two interesting aspects become obvious in this context. Firstly, the interspecies hybrid *O. kuroiwai* (*O. pumila* × *O. liukiuensis*) showed an intermediate CPT production in the roots in respect to *O. pumila* and *O. liukiuensis* that speaks for a genetically determined constitutive CPT production. Secondly, *O. kuroiwai* showed through its higher CPT levels per flask with a higher growth rate the growth-related biosynthesis of CPT. López-Meyer and Nessler (1997) were able to show that in *C. acuminata*, two autonomously regulated genes for the tryptophan decarboxylase (TDC), one of the key enzymes in the CPT biosynthesis, are present. One copy (*tdc1*) is expressed developmentally in the young tissues, and the other one (*tdc2*) is part of a defence system induced by pathogens. Yamazaki et al. (2003a) found that in *O. pumila*, two encoding genes are presumably also present. This may be the case in *O. mungos* too. In this context, our own intensive elicitor studies on transformed and untransformed root organ cultures show no induction of a significantly higher CPT biosynthesis besides a small one induced by a combination of IAA and kinetin based on a slightly higher growth rate (cf. secs. 2.7 + 3.7). In this, a path of induction as described by the *tdc2*, as in *C. acuminata*, thus neither exists nor is active in *O. mungos*. Some elicitation tests performed in other studies showed partial inductions of the CPT biosynthesis in *Ophiorrhiza* species. An increase of the STR (strictosidine synthase) and TDC mRNA expression was shown for DMSO treatment of root cultures of *O. pumila* by Yamazaki et al. (2003a), but no significant rise in CPT biosynthesis in relation to water controls was detected. Asano et al. (2004) described an enhanced alkaloid production of about 1.3-fold by treatment of the hairy roots of *O. liukiuensis* with 100 μM methyl jasmonic acid (MeJA) based on a higher growth rate. Salicylic acid (SA) showed no effects. Deepthi and Satheeshkumar (2016, 2017a, b) investigated the CPT production in cell suspension and adventitious roots cultures of *O. mungos*. The nutrients ($AgNO_3$; yeast extract) and the MeJA affected the CPT yields in the cell suspension cultures, again proportionally to the growth rates. Plant growth regulators and nutrition tests in adventitious root cultures yielded the same results. Nagesha et al. (2018) reported studies on shoot cultures of *O. mungos*, again with MeJA and SA. The highest CPT yields were attained with 0.23% by treatment with 150 μM MeJA compared to untreated plants with 0.11%. SA failed again. Consequently, the available studies verify our assumption of a growth-related CPT biosynthesis in *O. mungos*.

To come back to the CPT localization and distribution in the plant root and root cultures of *O. mungos*, it can be speculated that some patterns can also be a result of transport phenomena. A systemic transport of CPTs in *O. mungos* was ruled out, because we never detected any CPT fluorescence in the vascular bundles. Additionally, the plants had to fight over years against mealy bugs and aphids in the greenhouse, and these pests loved our *O. mungos* cultures (Fig. 9b). Even the analysis of the mealy bugs from *O. mungos* showed no detectable content of CPTs. A short-distance transport of CPT can be considered in a closer inspection of the

cytosolic distribution in the calyptra and the rhizodermis of the root cultures, the partly cytosolic localization in the root-hair zone and the exodermis of the plant root, the shift of the CPT between the cell layers at the border of rhizodermis and exodermis, and of course of the release in the outer medium. Sirikantaramas et al. (2007b) carried out studies on the questions of inter- and intracellular transport mechanisms and vacuolar storage of CPT in *O. pumila*. Here, an active transport was ruled out by inhibition tests of transporters and vesicle transport. A simple diffusion process was postulated with the finding that the CPT release was increased by blocking the vesicle transport. But, as we saw in our downstream experiments with resin, 60% of the CPT was still retained in the root tissue. As shown in the literature, hydrophilic secondary metabolites are usually stored in idioblasts and vacuoles (e.g. Shitan and Yazaki 2007) by protonation at lower pH. As Fassberger and Stella (1992) described in the case of CPT, the transformation from the lactone to the carboxylate form takes place at a pH ≥ 7 and in reverse at pH ≤ 7. At the cytosolic pH ($\approx$7), then, the CPT can be in both forms. The lactone form should be able to pass the tonoplast because it is highly lipophilic. But within the plant vacuole, the normal pH is around 5, and we know from our own studies that the vacuoles in the storage cells of the plant root of *O. mungos* are at a pH of 3.2 ± 0.2 (unpublished). At this pH, the lactone form will be formed and the CPT can leave the vacuole freely. A protonation of the nitrogen in the B-ring (cf. structure Fig. 17a) does not take place until pH 1–2 has been reached (cf. Fig. 14.2a in Wetterauer et al. 2018). Furthermore, the bottleneck enzymes of the CPT biosynthesis are located in different compartments. The TDC is described as a cytosolic enzyme and the STR as a vacuolar one (Contin et al. 1999). In contrast, based on the data of Yamazaki et al. (2003a), who defined a vacuolar STR, a STR in the endoplasmic reticulum (ER) was proposed by Sirikantaramas et al. (2007b). The following description perhaps can be given. The CPT biosynthesis ends, in whatever way, in the ER and the CPT is transferred by vesicles into the vacuole. In the vacuole, the CPT is stored (partly?), in some way ever, or it disperses passively in respect to its physical and chemical properties (partly?). In sum, we cannot explain all the findings, but we conclude again that a combination of diffusion, as described by Sirikantaramas et al., and a kind of unknown storage process exists for the vacuolar storage, such as an attached pacing of several CPT molecules or non-covalent clustering with other vacuolarly stored molecules or something else. In the case of the cytosolic localizations, we have to mention that the emission spectrum of NADPH shows similar maxima as CPT. Therefore, the fluorescence in these regions should not be attributed to the CPT in total. A third mode of CTP localization and storage, which has not been discussed so far, can take place in the appropriate intercellular matrices in the roots. This can lead to additional effects on the physical and chemical equilibria in respect to a passive diffusion process. As we can see, e.g. in Fig. 15c, fluorescence in these parts becomes obvious too. This can originate from cell wall components as well as from CPT. So CPT localization and also storage cannot be ruled out in these areas. Based on the known lower pH in the apoplast, an attached packing, as contemplated for the vacuoles, can happen. A non-covalent association with, e.g. polyphenols can also not be ruled out (comp. Roberts and Wink 1998).

A very important aspect is the function of the CPTs in *O. mungos* and its self-protection against them. In general, as mentioned above, the CPTs in the aerial parts seem to have a protective function against herbivores in relation to their localization. Additionally, the plant itself may have self-protection against the CPTs by a mutation of the topoisomerase I, as found for *C. acuminata*, *O. pumila*, and *O. liukiuensis* by Sirikantaramas et al. (2008). And for the case of a CPT release by wounding, we hypothesize that the calcium oxalate has a border function by inclusion of the CPTs to avoid a systemic dispersal (cf. Pasqua et al. 2004). Thus, the localization of the calcium oxalate next to the vascular bundles would make sense, apart from the calcium oxalate itself having a protective function against herbivores (Franceschi and Nakata 2005). In the root, the matter is different. Firstly, the root exhibits no calcium oxalate crystals. Secondly, the CPT is only localized in the dermata in the plant root, and therefore only a protection against small herbivores seems possible. Here, the release of CPT into the rhizosphere seems to be the important protection mode, something known from many root organ cultures of CPT-producing plants. This can have an allelopathic reason, such as the defence of resources in relation to other plants (growth regulator) or to keep insects and other vermin away (e.g. Saito et al. 2001). In the case of *O. mungos*, we did not investigate the soil of the plant root for its CPT content, but in sterile plant cultures with roots, we saw a clear CPT fluorescence in the culture agar, so that it has to be assumed that the plant root releases CPT into the soil too. The mode of the CPT release from the plant root is still unclear. Also, for the root organ cultures, the modes of storage and release, or better of outer content regulation, are still not known. Sirikantaramas et al. (2007b) showed for *O. pumila* that the release probably is mainly mediated by passive diffusion. With respect to our aim of large-scale production of CPT with root organ cultures in biofermenters, the item of CPT medium content regulation is so important that we had a closer look for *O. mungos* root cultures. First, we recognized over the years that the different root culture lines exhibit quite strict CPT contents in the culture medium, depending on the line. For example, the untransformed root organ culture kept a CPT content of approx. 12.6 µM and the transformed line 607 of approx. 5.2 µM (cf. Wetterauer et al. 2018). That should be a hint that the outer concentration is actively regulated at first sight. The release can happen by the loss of CPT-containing cells of the calyptras through normal growth and, as shown in the case of the root exudates, by leaking out. However, after refreshing the root culture medium, the growth of the roots takes some time to continue, because of the stress through the changed surrounding. However, the CPT contents in the medium are at the same level after the first 48 h, and, for a short time, even higher, followed by a quick downregulation to the line-dependent level. At the same time, the relative and absolute CPT contents in the root tissues show an inverse behaviour. Again, the one observation speaks for a passive content regulation and the other for an active one. We thus continued to research in two directions (none of the following results are shown here). Firstly, we did downstream experiments by resins to remove all CPT from the culture medium (comp. Saito et al. 2001), with the result that slight growth induction in the roots was observed to compensate the loss of CPT, but in the end, the root tissue contents became adjusted to a lower but

constant level of about 60% of the normal one. This is parallel to the results of Saito et al. (2001) for similar tests on root cultures of *O. pumila*. Secondly, we added CPT in quantities up to 5 mg per flask. All CPT was taken up by the roots until the natural medium concentration was reached again. Under UV light (366 nm), these root cultures showed an amplified CPT fluorescence. To rule out that the CPT only attached to the root surface, we did confocal microscopy studies and saw that the CPT fluorescence was stronger in the same regions in which the CPT was stored normally. After that we added resin in turn, again all the added CPT was removed, and the CPT content went down anew to the same constant level as in the first downstream experiment. On the one hand, the results show again a partly passive regulation; on the other hand, we see the stable, albeit lesser, remnant of the tissue CPT content that was not depleted by the resin. Further on, we performed a competitive uptake experiment with the structurally related ajmalicine. Here, we added 3 mg of CPT and the same amount of CPT combined with the equivalent dose of ajmalicine. As a result, the relative uptake of CPT was reduced by a sixth in the combination with ajmalicine, giving no further hint of a differentiation between active and passive regulations. Last of all, we tested an addition of 9-methoxy CPT, which is not synthesized in the roots. As mentioned, both metabolites, CPT and 9-methoxy CPT, have the same excitation wavelength, but different emission wavelengths (sec. 2.4). By two-photon excitation microscopy, we tried to determine the disposition of the 9-methoxy CPT within the living root tissue. As a result, we were able to verify uptake of 9-methoxy CPT, but failed in determining the localization due to the resolution. In sum, we have not been able to understand the mode of CPT content regulation so far, but we assume that here a combination of passive diffusion and another type of storage (physically or chemically) takes place.

To clarify the complex regulation of CPT biosynthesis, storage, and ecological function a little more, perhaps a closer look at the photosynthetic tissues will give further hints. In our basic studies on green roots (untransformed roots under light explosion, q.v. Flores et al. 1993), we noticed that the biosynthesis of CPTs is comparable to the aerial parts. Not only does the biosynthesis of 9-methoxy CPT start (cf. Fig. 14.1 in Wetterauer et al. 2018 and Fig. 3), but also suddenly a high content of strictosamide occurs in the extracts of the green roots, which is not present in the normal untransformed root culture cultured in the dark. Hence, on the one hand, the green roots show that the biosynthesis of 9-methoxy CPT is related in some way to the photosynthetic metabolism (cf. Chang et al. 2019) and, on the other hand, that maybe another regulation of the biosynthesis or reaction mode in relation to environmental factors will take part due to the occurrence or storage of precursor metabolites in the green tissues at a high level.

As mentioned before, the biosynthetic pathways of the CPT and derivative biosynthesis in the producing plants have so far not been fully elucidated, and so the biotechnological possibilities for an in vitro production are minimal at the moment. Another interesting new field in finding alternative ways for CPT production in the future maybe are endophytic fungi and bacteria from CPT-producing plants that could biosynthesize CPT as well (comp. Wetterauer et al. 2018).

Cell culture systems have failed until now due to their low biosynthetic performance. Therefore, root organ culture systems are the most realistic and economically possible way to mass-produce CPT at the moment, besides the classical plantation. Robust data on the worldwide demand for CPT are hard to obtain. As listed in Wetterauer et al. (2018), Asano et al. (2004) give 1000 kg CPT, based on derivative demands for chemotherapy. Since 2014, the demand for CPT has been quoted at 3000 kg, but without any given sources (Cui et al. 2015; Kai et al. 2014; Raveendran 2015). In contrast, Kai et al. (2014) give an annual worldwide CPT production of 600 kg, whereas our own enquiry in 2013 resulted in a delivery capacity of 1000 kg/month (only one supplier!). Even if the data given are inconsistent, in respect of greater independence from the producing countries and for a more sustainable bio-production, the fermenter technology of root organ cultures represents a good alternative. To confirm this, we want to do a little estimation. As Li and Adair (1994) wrote, a three-year-old tree of *C. acuminata* contains 50 mg of CPTs; on their assumption that 30% of the cancer patients in the United States are treated with CPT and each patient needs about 1–3 g CPT, they calculated that 7–21 million young trees are needed annually on 4200–12,600 hectares of plantations. That corresponds to approx. 350–1000 kg CPT. In our untransformed root organ cultures, 50 mg CPT corresponds to 20–25 g tissue produced in 2 weeks by 10–15 cultures. To produce 1 kg of CPT, 500 kg of root tissue is necessary. This seems a great deal, but in a suitable large-scale fermenter, a cultivation of 25–50 kg of roots/fermenter should be possible within a few weeks. When using 100 fermenters, a production of 10 kg CPT should be possible in 2 months (≥35,000 € value) and in 1 year about 60 kg with a value of over 200,000 €. But a single batch production can be increased by online downstream processing of the CPT out of the culture medium without harvesting the tissue, because up to 40% of the synthesized CPT can be released by the roots into the culture medium, as mentioned above. In this connection, the downstream processing and purification of the CPT can take place by means of resin or semipermeable membranes with little labour and expense. Additionally, by light exposure, the untransformed roots of *O. mungos* turn green and produce 9-methoxy CPT that is twice as expensive as normal CPT. The real productivity of such a fermenter system cannot be specified exactly without more experience. In the present study, we demonstrate the important factors of the upscaling process. Here especially the composition of the culture medium, the inoculum size and its dispersion on the carrier system, and the sterility, besides the technical challenges, are pointed out (sec. 2.8). In two fermenter runs with transformed and untransformed root organ cultures of *O. mungos*, we highlighted the behaviour of the root system, which was close to the root shaking cultures, and we were able to show the CPT post-production of the root batches after a little downstream with resin and after medium exchange (sec. 3.8). Of course, we reached no enormous CPT medium content (≈1 mg/l) in this little fermentation scale here, but firstly, we did not use the most productive root lines for our basic studies, and secondly, on a larger scale, the CPT production will come into a more commercial range, as the former ROOTec company was able to show. Nevertheless, every kg of CPT produced by fermenter technology saves at least 12 hectares of plantations or natural resources. The

purification of the CPTs is quite simple and cheap and does not contaminate the environment. Consequently, it would be a feasible and sustainable method of CPT production as raw material for the chemical industry that can fill supply shortages and save environmental resources in the actual producing countries.

5 Conclusions

The pathway of the CPT biosynthesis in the producing plants has as yet not been completely elucidated. The storage and release of CPT in the different plant organs still pose basic questions too. For *O. mungos*, we were able to show a constitutive and developmentally regulated CPT biosynthesis. Extensive elicitation studies on root organ cultures did not lead to an amplification of the CPT biosynthesis. The vacuolar storage in the aerial parts of the plant exhibits a distribution pattern of CPTs against herbivores with the highest concentrations in the inflorescences and the young leaves. Here, mainly 9-methoxy CPT is biosynthesized, probably with the participation of enzymes related to the photosynthesis apparatus. In the roots, only CPT is biosynthesized and partly released in the surroundings, probably for allelopathic reasons, such as plant growth regulation. Here, the CPT is vacuolarly and cytosolically localized in the epidermis. In the root organ cultures, CPT is dispersed equally in relation to the dry weight, which confirms again a constitutive and growth-regulated CPT biosynthesis in *O. mungos*. In this context, the different CPT content levels in the culture lines are probably genetically determined in a previously unknown way.

Focussing on the biotechnological CPT production, root organ cultures seem to be the only feasible way to produce CPT economically in relation to the classical plantations at the moment. In root organ cultures of *O. mungos*, the CPT contents are at the same or even higher levels as in the mother plant; CPT is partly released in the culture medium, and the downstream processing and purification is quite easy. Therefore, the root fermenter technology is a sustainable method of CPT production to save natural and environmental resources. Also, a higher independence from the CPT-producing countries will be achieved and CPT supply shortages in the demand of the chemical industry for this high-value and medicinally important secondary metabolite can be filled.

Acknowledgements This work was supported by a grant of the German Federal Ministry of Education and Research (BMBF, 0312739). For providing an adult plant of *O. mungos*, we thank Dr. M. Schwertfeger and Mr. J. Lautner of the Old Botanical Garden of Göttingen, Germany. For support in the cultivation regime of the root organ cultures and plants of *O. mungos*, we thank Mrs. H. Staudter (IPMB) and the staff of the Botanical Garden of Heidelberg, especially Mr. H. P. Hilbert. Thanks also to Dr. J. Gonzales (formerly IPMB) for graphical support in generating the drawings in Figs. 17 and 19 and Dr. A. Holloschi (Faculty of Biotechnology, HS Mannheim) for the perforamance of the two-photon excitation microscopy. For the support in the construction of the test root mist fermenter WEWA I, we thank the staffs of the precision engineering workshop and the glass-blowing workshop of the DNF-Werkstattverbund Neuenheimer Feld, Heidelberg University, in particular to Mr. F. Weidner, Mr. G. Hofmann, Mr. J. Karrer, Mr. N. Schmutz, and Mrs. U. Scheurich. We thank Dr. P. Ripplinger (CEO, ROOTec GmbH) for his generous support.

References

Agarwal KP, Dhar MM (1959) Chemical examination of *Ophiorrhiza mungos* Linn. J Sci Ind Res 18B:114–115

Anaswara Krishnan S, Dileepkumar R, Nair AS, Oommen OV (2014) Studies on neutralizing effect of *Ophiorrhiza mungos* root extract against *Daboia russelii* venom. J Ethnopharmacol 151:543–547

Asano T, Watase I, Sudo H, Kitajima M, Takayama H, Aimi N, Yamazaki M, Saito K (2004) Camptothecin production by *in vitro* cultures of *Ophiorrhiza liukiuensis* and *O. kuroiwai*. Plant Biotechnol 21:275–281

Asano T, Kobayashi K, Kashihara E, Sudo H, Sasaki R, Iijima Y, Aoki K, Shibata D, Saito K, Yamazaki M (2013) Suppression of camptothecin biosynthetic genes results in metabolic modification of secondary products in hairy roots of *Ophiorrhiza pumila*. Phytochemistry 91:128–139

Bastian P, Bauer J, Chavarría-Krauser A, Engwer C, Jäger W, Marnach S, Ptashnyk M, Wetterauer B (2008) Modelling and simulation of hairy root growth. In: Krebs H-J, Jäger W (eds) Mathematics – key technology for the future. Springer, Berlin, Heidelberg, pp 101–115

Beegum AS, Martin KP, Zhang C-L, Nishitha IK, Ligimol SA, Madhusoodanan (2007) Organogenesis from leaf and internode explants of *Ophiorrhiza prostrata*, an anticancer drug (camptothecin) producing plant. Electron J Biotechnol 10:114–123

Buta JG, Worley JF (1976) Camptothecin, a selective plant growth regulator. J Agric Food Chem 24:1085–1086

Chang C, Liu Z, Wang Y, Tang Z, Yu F (2019) A bZIP transcription factor, CaLMF, mediated light-regulated camptothecin biosynthesis in *Camptotheca acuminata*. Tree Physiol 39:372–380

Contin A, van der Heijden R, Verpoorte R (1999) Localization of secologanin in *Cantharanthus roseus* cells. Acta Bot Gallica 146:105–110

Cui L, Ni X, Ji Q, Teng X, Yang Y, Wu C, Zekria D, Zhang D, Kai G (2015) Co-overexpression of geraniol-10-hydroxylase and strictosidine synthase improves anti-cancer drug camptothecin accumulation in *Ophiorrhiza pumila*. Sci Rep 5:8227

Darwin SP (1976) The pacific species of *Ophiorrhiza* L. (Rubiaceae). Lyonia 1:47–102

De Luca V, St Pierre B (2000) The cell and developmental biology of alkaloid biosynthesis. Trends Plant Sci 5:168–173

Deepthi S, Satheeshkumar K (2016) Enhanced camptothecin production induced by elicitors in the cell suspension culture of *Ophiorrhiza mungos* Linn. Plant Cell Tissue Organ Cult 124:483–493

Deepthi S, Satheeshkumar K (2017a) Cell line selection combined with jasmonic acid elicitation enhance camptothecin production in cell suspension cultures of *Ophiorrhiza mungos* L. Appl Microbiol Biotechnol 101:545–558

Deepthi S, Satheeshkumar K (2017b) Effects of major nutrients, growth regulators and inoculums size on enhanced growth and camptothecin production in adventitious root cultures of *Ophiorrhiza mungos* L. Biochem Eng J 117:198–209

Fassberger J, Stella VJ (1992) A kinetic and mechanistic study of the hydrolysis of camptothecin and some analogues. J Pharma Sci 81:676–684

Flores HE, Y-r D, Cuello JL, Maldonado-Mendoza IE, Loyola-Vargas VM (1993) Green roots: photosynthesis and photoautotrophy in an underground plant organ. Plant Physiol 101:363–371

Flores HE, Vivanco JM, Loyola-Vargas VM (1999) 'Radical' biochemistry: the biology of root-specific metabolim. Trends Plant Sci 4:220–225

Franceschi VR, Nakata PA (2005) Calcium oxalate in plants: formation and function. Annu Rev Plant Biol 56:41–71

Gamborg OL, Miller RA, Ojima K (1968) Nutrient requirement of suspensions cultures of soybean root cells. Exp Cell Res 50:151–158

Hooker JD (1882) The flora of British India Vol. III. L Reeve & Co, London, p 77

Hsiang Y-H, Hertzberg RP, Hecht SM, Liu LF (1985) Camptothecin induces protein-linked DNA breaks via mammalian DNA Topoisomerase I. J Biol Chem 260:14873–14878

Kai G, Teng X, Cui L, Li S, Hao X, Shi M, Yan B (2014) Effect of three plant hormone elicitors on the camptothecin accumulation and gene transcript profiling in *Camptotheca acuminata* seedlings. Int J Sci 3:86–95

Kirtikar KR, Basu BD (1975) Indian medicinal plants Vol. II, 2nd edn. M/S Bishen Singh Mahendrapal Singh, New Delhi, pp 1267–1269

Li S, Adair KT (1994) XI SHU, a promising anti-tumor and anti-viral tree for the 21st century. A Henry M. Rockwell monograph. The Tucker Center, College of Forestry, Stephen F. Austin State University, Nacogdoches

Liu Z, Adams J (1996) Camptothecin yield and distribution within *Camptotheca acuminata* trees cultivated in Louisiana. Can J Bot 74:360–365

Liu Z, Adams JC, Viator HP, Constantin RJ, Carpenter SB (1999) Influence of soil fertilization, plant spacing and coppicing on growth, stomatal conductance, abscisic acid and camptothecin levels in *Camptotheca acuminata* seedlings. Physiol Plant 105:402–408

Liu Y-Q, Li W-Q, Morris-Natschke SL, Qian K, Yang L, Zhu G-X, Wu X-B, Chen A-L, Zhang S-Y, Nan X, Lee K-H (2015) Perspectives on biologically active camptothecin derivatives. Med Res Rev 35:753–789

López-Meyer M, Nessler CL (1997) Tryptophan decarboxylase is encoded by two autonomously regulated genes in *Camptotheca acuminata* which are differentially expressed during development and stress. Plant J 11:1167–1175

López-Meyer M, Nessler CL, McKnight TD (1994) Sites of accumulation of the antitumor alkaloid camptothecin in Camptotheca acuminata. Planta Med 60:558–560

Madhavan V, Yoganarasimhan S, Gurudeva M, John CR, Deveswaran R (2013) Pharmacognostical studies on the leaves of *Ophiorrhiza mungos* Linn. (Rubiaceae). Spatula DD 3:89–98

Nadkarni KM (1927) The Indian Materia Medica. Presidency Printing Press, Bombay, pp XI + 615–616

Nagesha BV, Amilineni U, Gudasalamani R, Karaba NN, Ramanan US (2018) Elicitors act as a signal transducer in the enhancement of camptothecin production from in vitro cultures of *Ophiorrhiza mungos* L. Ann Phytomed 7:46–54

Oberlies NH, Kroll DJ (2004) Camptothecin and Taxol: historic achievements in natural products research. J Nat Prod 67:129–135

Pasqua G, Monacelli B, Valletta A (2004) Cellular localisation of the anti-cancer drug camptothecin in Camptotheca acuminata Decne (Nyssaceae). Eur J Histochem 48:321–328

Quisumbing E (1978) Medicinal plants of the Philippines. Katha Publishing Co, Manila, p 922

Raveendran VV (2015) Camptothecin-discovery, clinical perspectives and biotechnology. Nat Prod Chem Res 3:175

Renjith R, Sibi CV, Rajani K, Roja G, Venkataraman R, Satheeshkumar K, Sabulal B (2013) Search for camptothecin-yielding *Ophiorrhiza* species from southern Western Ghats in India: a HPTLC-densitometry study. Ind Crop Prod 43:472–476

Renjith R, Sibi CV, Rajani K, Roja G, Venkataraman R, Satheeshkumar K, Sabulal B (2016) HPTLC-based quantification of camptothecin in *Ophiorrhiza* species from southern Western Ghats in India. Cogent Chem 2:1275408

Roberts MF, Wink M (1998) Alkaloids. Plenum Press, New York

Roja G (2006) Comparative studies on the camptothecin content from *Nothapodytes foetida* and *Ophiorrhiza* species. Nat Prod Lett 20:85–88

Saito K, Sudo H, Yamazaki M, Koseki-Nakamura M, Kitajima M, Takayama H, Aimi N (2001) Feasible production of camptothecin by hairy root culture of *Ophiorrhiza pumila*. Plant Cell Rep 20:267–271

Sanyal D (1984) Vegetable drugs of India. Bishen Singh Mahendra Pal Singh, Dehra Dun, pp 169–170

Shitan N, Yazaki K (2007) Accumulation and membrane transport of plant alkaloids. Curr Pharm Biotechnol 8:244–252

Sirikantaramas S, Asano T, Sudo H, Yamazaki M, Saito K (2007a) Camptothecin: therapeutic potential and biotechnology. Curr Pharm Biotechnol 8:96–202

Sirikantaramas S, Sudo H, Asano T, Yamazaki M, Saito K (2007b) Transport of Camptothecin in hairy roots of *Ophiorrhiza pumila*. Phytochemistry 68:2881–2886

Sirikantaramas S, Yamazaki M, Saito K (2008) Mutations in topoisomerase I as a self-resistance mechanism coevolved with the production of the anticancer alkaloid Camptothecin in plants. PNAS 105:6782–6786

Tafur S, Nelson JD, DeLong DC, Svoboda GH (1976) Antiviral components of *Ophiorrhiza mungos* isolation of camptothecin and 10-methoxycamptothecin. Lloydia 39:261–262

Thwaites GHK (1864) Enumeratio Plantarum Zeylaniae. Dulau & Co, London, p 139

von Linne' C (1753) Species Plantarum, Volume I. Impensis Laurentii Salvii, Holmiae, p 150

Wall ME, Wani MC, Cook CE, Palmer KH (1966) Plant antitumor agents. I. The isolation and structure of camptothecin, a novel alkaloidal leukemia and tumor inhibitor from *Camptotheca acuminata*. J Am Chem Soc 88:3888–3890

Wang CY, Buta JG, Moline HE, Hruschka HW (1980) Potato sprout inhibition by camptothecin, a naturally occurring plant growth regulator. J Am Soc Hortic Sci 105:120–124

Wang X, Tanaka M, Krstin S, Peixoto HS, de Melo Moura CC, Wink M (2016) Cytoskeletal interference – a new mode of action for the anticancer drugs camptothecin and topotecan. Eur J Pharmacol 789:265–274

Wetterauer B (2008) Produktion von Camptothecin in *Ophiorrhiza mungos* – Pflanzen, Organkulturen und fermentation. Dissertation, Ruprecht-Karls-Universität of Heidelberg

Wetterauer B, Wildi E, Wink M (2018) Production of the anticancer compound camptothecin in root and hairy root cultures of *Ophiorrhiza mungos* L. In: Kumar N (ed) Biotechnological approaches for medicinal and aromatic plants – conservation, genetic improvement and utilization. Springer-Nature, Singapore, pp 303–341

Wink M (1988) Plant breeding: importance of plant secondary metabolites for protection against pathogens and herbivores. Theor Appl Gen 75:225–233

Wink M (2003) Evolution of secondary metabolites from an ecological and molecular phylogenetic perspective. Phytochemistry 64:3–19

Wink M, Wetterauer B (2019) Biotechnologische Produktion biogener Wirkstoffe – Wurzelkulturen als Produktionssystem. BIOspektrum 25:455–457

Wink M, Alfermann AW, Franke R, Wetterauer B, Distl M, Windhoevel J, Krohn O, Fuss E, Garden H, Mohagheghzadeh A, Wildi E, Ripplinger P (2005) Sustainable bioproduction of phytochemicals by plant in vitro cultures: anticancer agents. Plant Genet Resour-C 3:90–100

Yamazaki Y, Sudo H, Yamazaki M, Aimi N, Saito K (2003a) Camptothecin biosynthetic genes in hairy roots of *Ophiorrhiza pumila*: cloning, characterisation and differential expression in tissues and by stress compounds. Plant Cell Physiol 44:395–403

Yamazaki Y, Urano A, Sudo H, Kitajima M, Takayama H, Yamazaki M, Aimi N, Saito K (2003b) Metabolite profiling of alkaloids and strictosidine synthase activity in camptothecin producing plants. Phytochemistry 62:461–470

Yamazaki M, Mochida K, Asano T, Nakabayashi R, Chiba M, Udomson N, Yamazaki Y, Goodenowe DB, Sankawa U, Yoshida T, Toyoda A, Totoki Y, Sakaki Y, Góngoora-Castillo E, Buell CR, Sakurai T, Saito K (2013) Coupling deep transcriptome analysis with untargeted metabolic profiling in *Ophiorrhiza pumila* to further the understanding of the biosynthesis of the anti-cancer alkaloid camptothecin and Anthraquinones. Plant Cell Physiol 54:686–696